DEUTSCHES ELEKTRONEN-SYNCHROTRON **DESY**

DESY 88-095
MZ-TH/88-09
July 1988

QCD JETS AT HERA

I. O( ) RADIATIVE CORRECTIONS TO ELECTROWEAK CROSS SECTIONS AND JET RATES

by

J.G. Körner, E. Mirkes

Inst. f. Physik, Johannes-Gutenberg-Univ., Mainz

G.A. Schuler

Deutsches Elektronen-Synchrotron DESY, Hamburg

ISSN 0418-9833

NOTKESTRASSE 85 · 2 HAMBURG 52

To be sure that your preprints are promptly included in the
HIGH ENERGY PHYSICS INDEX ,
send them to the following address (if possible by air mail) :

DESY
Bibliothek
Notkestrasse 85
2 Hamburg 52
Germany

DESY 88-095 ISSN 0418-9833

MZ-TH /88-09

July 1988

QCD Jets at HERA
I. $O(\alpha_s)$ Radiative Corrections to Electroweak Cross Sections and Jet Rates

Jürgen G. Körner and Erwin Mirkes

Inst. f. Physik, Johannes Gutenberg-Universität, Mainz

Gerhard A. Schuler

Deutsches Elektronen-Synchrotron DESY, Hamburg

Abstract

We present the complete $O(\alpha_s)$ corrections to the electro-weak cross sections of both neutral current and charged current deep inelastic $e^{\pm}p$ scattering including lepton polarization effects. Changes in the cross section due to the inclusion of next-to-leading-log (NLL) effects are parametrized by K-factors, which are defined as the ratio of the NLL $O(\alpha_s)$ cross sections and the Born cross section. Using the standard redefinition scheme of the parton densities, we find that the K-factors deviate substantially from unity for small values of the Bjorken-Scaling variable x. We also elaborate on problems that arise when defining jet cross sections in ep scattering and present numerical results for the $O(\alpha_s)$ 3-jet and 2-jet rates. We observe that the Q^2-dependence of the 3-jet rate is dominated by the running strong coupling constant $\alpha_s(Q^2)$ allowing for its determination over a wide range in Q^2 at high energy ep colliders.

1 Introduction

Up to now QCD has been succesfully tested in high energy e^+e^- and $p\bar{p}$ collisions. The limited energy available at the existing fixed target leptoproduction experiments at CERN and at Fermilab make it much harder at present to observe QCD effects in leptoproduction. The new storage ring HERA will provide collisions between 30 GeV electrons and 820 GeV protons. At these high energies one can expect large QCD effects [BIS87]. In this paper we consider the complete $O(\alpha_s)$ QCD corrections to deep inelastic ep scattering. Higher order QCD corrections are important for several reasons. Firstly, they give rise to a rescaling of the absolute cross section relative to that predicted from the usual leading log (LL) QCD phenomenology, i.e. they give rise to a K-factor. Secondly, they influence the structure of the hadronic system. This includes overall event properties, jet multiplicities and widths, momentum distributions, as well as energy flow and correlations. While parton cascade approaches are in competition with the fixed order matrix elements method in "predicting" the event structure in leptoproduction, they fail to provide the overall cross section normalization. Furthermore, fixed order perturbative QCD calculations allow a *prediction* of the rate of low multiplicity jet events. For example to lowest order in $O(\alpha_s^0)$ the hadronic system is a two jet event which consist of the struck quark jet and the proton remnant jet. To $O(\alpha_s)$ one can have three jet event final states. In general, parton cascade models will not yield the right ratio of e.g. the 3-jet events to 2-jet events. Parton cascade models should be matched with the exact $O(\alpha_s)$ formula once these are known. This can e.g. be done by using a rejection procedure similar to the one that was succesfully used in the e^+e^- case [BS87]. Finally, detailed tests of QCD can only be performed using the *full* QCD matrix elements which may lead yet to another determination of the running QCD coupling constant α_s.

The calculation of the $O(\alpha_s)$ corrected electro-weak cross section of deep inelastic lepton-proton scattering consists of three steps. Firstly, the $O(\alpha_s)$ partonic cross sections have to be calculated. The next step consists in the redefinition of the parton densities to $O(\alpha_s)$. This is a consequence of the fact that initial state mass singularities remain at the level of the perturbative parton cross sections in contradistinction to the e^+e^--case. They have to be absorbed by a suitable renormalization of the parton densities. This in turn implies that the actual form and magnitude of the $O(\alpha_s)$ corrected cross section does depend on the choice of redefinition scheme. Since there are subtle points involved in this redifinition we feel it necessary to recapitulate this connection in some detail. In deep inelastic lepton hadron scattering it is most natural to apply the "standard scheme" which is defined by requiring that the form of the structure function F_2 is preserved to all orders of perturbation theory [AEM79]. The perturbative $O(\alpha_s)$ corrections are small over most of the available phase space region, yet they give rise to some interesting physics in the very small x region which we discuss in some detail.

The last step in the calculation of the $O(\alpha_s)$ leptoproduction cross section is the inclusion of electro-weak model dependencies as well as the inclusuion of longitudinal polarization effects of the incoming electron or positron beam. We present twice differential $O(\alpha_s)$ cross section formula $d^2\sigma/(dxdy)$ both for neutral current and charged current electron (positron) proton scattering including beam polarization effects. Some of the formulas are new.

We determine neutral current and charged current K-factors, which are defined as the ratio of the $O(\alpha_s)$ corrected cross section and the corresponding lowest order Born

cross section. The K-factors are in general x- and y-dependent and thus may change the overall event characteristic as well as the overall normalization of the cross section. We note that the present leptoproduction Monte Carlo generators do not include the effects of K-factors which we find to deviate substantially from unity for very small values of x. The quatitative analysis of the K-factor allows one to deliniate a boundary in the (x, Q^2)-plane beyond which no reliable QCD predictions can be made that are based on the standard LL Altarelli-Parisi evolution analysis.

Several event characteristics have been proposed to test the higher order perturbative QCD corrections. $O(\alpha_s)$ predictions have been made for the infrared/collinear (IR/M)-safe average values of thrust $< T >$ and sphericity $< S >$ [S156], and the leptoproduction averaged transverse momentum $< p_T^2 >_{jet}$ [AM78, Mo81]. IR/M safe measures are also provided by the energy flow and the energy correlations [PR80]. The obvious disadvantage is that these mean values receive major contributions from those regions of the respective variable where nonperturbative effects are likely to bury the perturbative QCD contributions. Another procedure is to study distributions of global jet variables like $d\sigma/dS$, $d\sigma/dT$ etc., i.e. to look for the "perturbative tail" (at large S, low T) where the QCD results emerges from beneath an estimate of the non-perturbative, fragmentation effects [GS78, MW79, BG79, RR79, KR80, KR81].

Yet another way of testing the $O(\alpha_s)$ corrections is to study the ratio of 3-jet events to 2-jet events. While in $O(\alpha_s^0)$ (or in the naive quark parton model) only 2-jet events can occur, the $O(\alpha_s)$ processes also allow for 3-jet events, either by hard gluon radiation or by boson-gluon fusion into a quark-antiquark pair. When one introduces Sterman-Weinberg-like conditions [SW77] to define the resolvability of two partons one can set up a 3-jet region in the 3-parton phase space. Integrating the (4-dimensional) differential $O(\alpha_s)$ tree graph cross section over the 3-jet region results in the 3-jet cross section. The 3-jet ratio was calculated in this way in ref. [S150] where the total $O(\alpha_s)$ cross section was approximated by the $O(\alpha_s^0)$ QPM formula. Also the 2- and 3-jet Monte Carlo event generator of [In86] is based on this procedure where again the total $O(\alpha_s)$ cross section is approximated by the $O(\alpha_s^0)$ QPM formula.

In this paper we provide a detailed study of jet properties in leptoproduction including the next-to-leading log (NLL) effects using invariant mass jet criteria. As mentioned above this necessitates a discussion of the $O(\alpha_s)$ corrections to the total cross section together with a discussion of the redefinition of the parton densities. The calculated 2-jet and 3-jet rates depend on the choice of the redefinition ("renormalization") scheme. Secondly, in leptoproduction there are some problems in defining jets compared to the e^+e^- case. The main source of these difficulties lies in the fact that there is no unique mass scale which can be used to define the resolvability of two partons. Also, jet definition becomes dependent on the overall event kinematics specified by (x, y) or (x, Q^2). Moreover, contrary to the e^+e^- fragmentation picture, jet definition in leptoproduction does *not* isolate the quark and gluon jets from their production origins. We determine jet rates and jet widths using the complete $O(\alpha_s)$ matrix elements including the full electroweak structure. We comment on approximations which are necessary in order to reduce the complexity of the complete cross section to the parton cascade structure. Finally we investigate the question how well the running of the strong coupling constant can be seen in the 3-jet rate $R_3(x, Q^2)$ as one expects from the fact that $R_3(x, Q^2)$ is directly proportional to $\alpha_s(Q^2)$. To this end we investigate additional sources of Q^2-dependencies of R_3 such as arise from ambiguities due to various possible jet definition schemes.

The organization of the paper is as follows. In section 2 we introduce some basic kinematical relations. We review the $O(\alpha_s^0)$ cross section formulae and outline how to include the corrections due to the $O(\alpha_s)$ terms. We discuss the scheme used to renormalize the parton densities to $O(\alpha_s)$ and present complete $O(\alpha_s)$ corrected deep inelastic structure functions both for the NC and the CC case. We then go on to calculate the $O(\alpha_s)$ K-factors. In section 3 we present total differential 3-jet formula. Next we discuss the problems that arise when defining jets in leptoproduction and calculate the 3-jet and 2-jet ratios. The last section contains a short summary. We devote three appendices to the technical details of the $O(\alpha_s)$ calculations. In particular Appendix C includes a careful discussion of the calculation of the parity violating structure function F_3 within the dimensional regularization scheme (which we use throughout). The calculation of the parity violating structure function F_3 involves parity-odd fermion traces and thus one encounters the problem of how to deal with γ_5 or the totally antisymmetric tensor $\epsilon_{\alpha\beta\gamma\delta}$ in n dimensions [KKLS 85]. We have included the details of this calculation since to our surprise, we have not found a consistent dimensional regularization calculation of F_3 in the literature. Our results for F_3 agree with those given by [CFP80, FP82 FKL81, HK81].

The present paper is the first in a series of papers which are devoted to the study of QCD jet production effects in leptoproduction. In the forthcoming papers we plan to discuss $O(\alpha_s^2)$ tree graph and loop effects. The scope of the technical material that we present in the appendices and, for that matter, also in the main text is already geared toward these higher order calculations.

2 Electroweak cross sections up to $O(\alpha_s)$

Consider deep inelastic electron (positron) proton scattering (X is an arbitrary hadronic final state)

$$e^{\pm}(l) + p(P) \to e^{\pm}(l') + X(P_f) \tag{1}$$

The particle momenta are given within the brackets. In our discussion of the neutral current (NC) process (1) we include both electromagnetic and weak neutral current contributions including parity-violating effects. Furthermore we allow the incoming lepton to have a longitudinal polarization ρ, where for unpolarized leptons $\rho = 0$ and for left-handed (right-handed) incoming leptons $\rho = -1$ ($\rho = +1$). In addition to the NC reaction (1) we have the charged current (CC) reaction

$$e^{\pm}(l) + p(P) \to (\overline{\nu})_e(l') + X(P_f) \tag{2}$$

which is mediated by the exchange of a $W^{\pm}$-boson. The CC reaction will be important for HERA energies [In87, Wo86]. However, since the partonic $O(\alpha_s)$ QCD calculations are the same both for the NC process (1) and the CC reaction (2), we will in the following discuss only the NC e^-p scattering case in detail. The results for the $O(\alpha_s)$ CC cross section are then added at the end of this section.

2.1 Quark Parton Model cross sections

Let us begin by establishing our notation for the kinematics. We denote the virtual photon/Z^0-boson ($W^{\pm}$-boson) momentum by q, the absolute value of its square by Q^2, the cms energy by s, the square of the final hadronic mass by W^2, and introduce scaling variables x and y. We have:

$$\begin{aligned} q &= l - l' \\ Q^2 &= -q^2 = xys \\ s &= (P+l)^2 \\ W^2 &= P_f^2 = (P+q)^2 \\ x &= \frac{Q^2}{2P\cdot q} \\ y &= \frac{P\cdot q}{P\cdot l} \end{aligned} \tag{3}$$

Note that for a given fixed s only two variables in eq. (3) are independent, since e.g. $xW^2 = (1-x)Q^2, Q^2 = xys$.

To lowest order $O(\alpha_s^0)$, or in the frame work of the naive quark parton model (QPM), the current is assumed to couple to a quark or antiquark with four-momentum $p = \eta P$ within the proton. (All particles are assumed to be massless.) Thus, in the case of e^-p scattering, the process (1) occurs via the partonic subprocesses depicted in Fig. 1a:

$$\begin{aligned} e^-(l) + q(p = \eta P) &\to e^-(l') + q(p') \\ e^-(l) + \bar{q}(p = \eta P) &\to e^-(l') + \bar{q}(p') \end{aligned} \tag{4}$$

In the QPM it turns out that the momentum fraction η of the proton momentum carried by the initial quark (antiquark) is nothing but the scaling variable x:

$$\eta[\mathrm{QPM}] = x \tag{5}$$

The leading log (LL) approximation to the QPM will lead to evolving parton densities. In this LL approximation the Callan-Cross relation $F_2[\mathrm{LL}](x,Q^2) = 2xF_1[\mathrm{LL}](x,Q^2)$ is still satisfied. As a consequence there is no contribution to the longitudinal structure function $F_L \equiv F_2 - 2xF_1$. At low Q^2 the pure γ-exchange term completely dominates the γ-Z interference and the pure weak term. In this pure QED case the cross section takes the familar form:

$$\frac{d^2\sigma^{\gamma}(e^-p)}{dxdy}[\mathrm{LL}] = \frac{2\pi\alpha^2}{xyQ^2}\, Y_+\, F_2^{\gamma}[\mathrm{LL}](x,Q^2) \tag{6}$$

The structure function F_2 can be expressed as a sum of quark (q_f) and antiquark ($\bar{q}_f$) densities

$$F_2^{\gamma}[\mathrm{LL}](x,Q^2) = \sum_{f=1}^{n_f} e_f^2 x\,[q_f(x,Q^2) + \bar{q}_f(x,Q^2)] \tag{7}$$

We have added the term LL in the brackets in order to emphasize the difference to the next to leading (NLL) stucture functions discussed in the following chapters. The sum in eq. (7) runs over all n_f light flavours within the proton. We denote by e_f the electric charge of the quark of flavour f ($e_u = +2/3$). The y-dependent factor Y_+ in eq. (6) is given by

$$Y_+ = 1 + (1-y)^2 \tag{8}$$

In ep colliders as HERA one can reach much higher values of Q^2 than in fixed target experiments (e.g. up to $Q^2 = 10^5\,\mathrm{GeV}^2$ at HERA). Then the $\gamma - Z$ term and the pure Z-exchange become more important and finally dominate the cross section in the upper Q^2-range [In87]. The weak effects are twofold: Firstly they modify the couplings of the quarks to the current, and, secondly, they cause another contribution to the cross section which is proportional to the difference of the quark and antiquark densities. This term, the structure function F_3, originiates from the parity-violating (p.v.) part of the hadronic squared matrix element, and its y-dependence is given by:

$$Y_- = 1 - (1-y)^2 \tag{9}$$

The NC cross section including these p.v. effects is given by:

$$\frac{d^2\sigma^{NC}(e^-p)}{dxdy}[\mathrm{LL}] = \frac{2\pi\alpha^2}{xyQ^2}\left\{Y_+\, F_2[\mathrm{LL}](x,Q^2) + Y_-\, x\, F_3[\mathrm{LL}](x,Q^2)\right\} \tag{10}$$

where now:

$$\begin{aligned} F_2[\mathrm{LL}](x,Q^2) &= \sum_{f=1}^{n_f} A_f(Q^2)\, x\,[q_f(x,Q^2) + \bar{q}_f(x,Q^2)] \\ x\,F_3[\mathrm{LL}](x,Q^2) &= \sum_{f=1}^{n_f} B_f(Q^2)\, x\,[q_f(x,Q^2) - \bar{q}_f(x,Q^2)] \end{aligned} \tag{11}$$

Taking the longitudinal polarization ρ of the incoming lepton into account, the electroweak factors are given by:

$$\begin{aligned} A_f(Q^2) &= e_f^2 + 2e_f v_f \Re(\chi_Z)(-v_e + \rho a_e) + (v_f^2 + a_f^2)\,|\,\chi_Z\,|^2\,(v_e^2 + a_e^2 - 2v_e a_e \rho) \\ B_f(Q^2) &= 2e_f a_f \Re(\chi_Z)(-a_e + v_e\rho) + 2v_f a_f\,|\,\chi_Z\,|^2\left(-2v_e a_e - \rho(v_e^2 + a_e^2)\right) \end{aligned} \tag{12}$$

Here $\chi_Z(Q^2)$ is the ratio of the Z^0-propagator to the photon propagator times a coupling strength factor:

$$\chi_Z(Q^2) = \frac{1}{(2\sin 2\theta_W)^2}\frac{Q^2}{Q^2 + m_Z^2 - im_Z\Gamma_Z} \tag{13}$$

The neutral current couplings in eq. (12) can be specified in a given electro-weak model. In the standard model one has:

$$\begin{aligned} v_e &= -1 + 4\sin^2\theta_W \quad , \quad a_e = -1 \\ v_f &= 2t_f - 4e_f\sin^2\theta_W \quad , \quad a_f = 2t_f \end{aligned} \tag{14}$$

where t_f denotes the third component of the weak isospin of the f-type quark ($t_u = +1/2$) and θ_W is the Weinberg angle.

For the sake of completeness we note that the NC e^+p cross section is obtained from eq. (10) by the replacements:

$$A_f(Q^2) \to A_f(Q^2) \quad ; \quad B_f(Q^2) \to -B_f(Q^2) \quad ; \quad \rho \to -\rho \tag{15}$$

2.2 $O(\alpha_s)$ corrections

To $O(\alpha_s)$ one has the virtual (loop graph) corrections to eq. (4) as well as the real (tree graph) massless parton contributions depicted in Fig. 1b–d: [1]

$$\begin{aligned} e^-(l) + q(p) &\to e^-(l') + q(p_1) + G(p_2) \\ e^-(l) + \bar{q}(p) &\to e^-(l') + \bar{q}(p_1) + G(p_2) \\ e^-(l) + G(p) &\to e^-(l') + q(p_1) + \bar{q}(p_2) \end{aligned} \tag{16}$$

Also heavy flavour production becomes possible in $O(\alpha_s)$ through boson-gluon fusion into heavy quark-antiquark pairs:

$$e^-(l) + G(p) \to e^-(l') + Q(p_1) + \bar{Q}(p_2) \tag{17}$$

The $O(\alpha_s)$ corrections modify the cross section eq. (10) in the following way: Firstly, there are nonzero contributions to the longitudinal structure functions F_L coming from the tree graphs (16). Since these terms originate from the parity conserving (p.c.) part of the hadronic squared amplitude they carry the same electro-weak dependence $A_f(Q^2)$ as does F_2. Secondly, there are contributions from the process (17) which yield heavy flavour structure functions $F_i[\mathrm{HF}](x,Q^2)$ for $i = 2, L, 3$. Note that both F_L and $F_i[\mathrm{HF}]$ start only at $O(\alpha_s)$. Finally, there are massless $O(\alpha_s)$ corrections to the structure functions F_2 and F_3. However, since these quantities already start at $O(\alpha_s^0)$, we do not only have to take into account the $O(\alpha_s)$ corrections to the partonic cross sections but we must also consider the $O(\alpha_s)$ corrections to the parton densities. As we shall discuss in the next subsection, the parton densities have to be redefined at $O(\alpha_s)$. Thus the $O(\alpha_s)$ corrections to F_2 and F_3 depend on the choise of redefinition scheme in much the same way as higher order loop corrections depend on the choice of renormalization scheme for the coupling constant.

[1] In order to be definite we again concentrate on the e^-p-case.

The complete $O(\alpha_s)$ cross section which includes next-to-leading log [NLL] effects will be denoted by the bracketed symbol [NLL]. The general form of the NLL $O(\alpha_s)$ corrected NC cross section is given by:

$$\begin{aligned} \frac{d^2\sigma^{NC}(e^-p)}{dxdy}[\mathrm{NLL}] = \frac{2\pi\alpha^2}{xyQ^2}\Big\{ & Y_+\, F_2[\mathrm{NLL}](x,Q^2) \;+\; Y_-\, x\, F_3[\mathrm{NLL}](x,Q^2) \\ & -\; y^2 F_L[\mathrm{NLL}](x,Q^2)\Big\} \end{aligned} \tag{18}$$

The [NLL] structure functions are sums of the LL contributions $F_i[\mathrm{LL}]$, the massless $O(\alpha_s)$ corrections $F_i[\alpha_s]$, and the $O(\alpha_s)$ heavy flavour terms $F_i[\mathrm{HF}]$:

$$\begin{aligned} F_2[\mathrm{NLL}](x,Q^2) &= F_2[\mathrm{LL}](x,Q^2) + \frac{\alpha_s}{2\pi}\Big[F_2[\alpha_s](x,Q^2) + F_2[\mathrm{HF}](x,Q^2)\Big] \\ x\,F_3[\mathrm{NLL}](x,Q^2) &= x\,F_3[\mathrm{LL}](x,Q^2) + \frac{\alpha_s}{2\pi}\Big[xF_3[\alpha_s](x,Q^2) + xF_3[\mathrm{HF}](x,Q^2)\Big] \\ F_L[\mathrm{NLL}](x,Q^2) &= \frac{\alpha_s}{2\pi}\Big[F_L[\alpha_s](x,Q^2) + F_L[\mathrm{HF}](x,Q^2)\Big] \end{aligned} \tag{19}$$

In the following, we suppress the term NLL in the brackets for the next to leading cross sections and structure functions whenever this omission does not lead to any misunderstanding.

The inclusion of the higher order QCD corrections does not only change the distributions in the kinematical variables x and y but also changes the overall cross section. The change of the cross section normalization is quantified by the K-factor which, to $O(\alpha_s)$, is defined as the ratio of the $O(\alpha_s)$ corrected NLL cross section and the Born (lowest order) cross section:

$$\frac{d^2\sigma}{dxdy}[\mathrm{NLL},\alpha_s] = K(x,Q^2)\,\frac{d^2\sigma}{dxdy}[\alpha_s^0] \tag{20}$$

However, before we can present results for the NC and CC K-factors, we have to define the scheme used to redefine the parton densities. This is the task of the next subsection.

2.3 Redefinition of parton densities in $O(\alpha_s)$

When calculating the $O(\alpha_s)$ corrected cross section of the light flavours, one is faced with the problem that mass singularities remain. This fact implies that the "bare" parton distributions $q_{0,i}(x)$ have to be "renormalized". Mass factorization tells us that all mass singularities may be factored from the perturbative partonic cross section and consistently absorbed into the parton distributions [EGMPR79, APV78, Mu78, LS78, FP82] which thereby acquire a calculable dependence on the scale size of the interaction (i.e. on Q^2 in DIS). However, the specific way in which this redefinition is done influences the sice of the $O(\alpha_s)$ corrections, i.e. determines the the magnitude of the "K-factor" for the ep cross section.

Let us first generalize the NLL cross section eq. (18) to $n = 4 - 2\epsilon$ dimensions. This is necessary since we control the ultraviolet (UV) and IR/M singularities that arise in intermediate steps of the calculations by use of dimensional regularization. Leaving the

contributions of the heavy flavour structure functions aside for the moment we find [2]:

$$\frac{d^2\sigma^{NC}}{dxdy}(e^-p) = K(\epsilon)\frac{2\pi\alpha^2}{Q^2y}\sum_{f=1}^{n_f}\left[A_f(Q^2)\left\{[Y_+ - \epsilon y^2]\mathcal{F}_2^f(x,Q^2) - y^2\mathcal{F}_L^f(x,Q^2)\right\}\right. \quad (21)$$
$$\left. + B_f(Q^2)\,Y_-\,\mathcal{F}_3^f(x,Q^2)\right]$$

For later convenience, we have also extracted the flavour sum by introducing the flavour dependent script structure functions $\mathcal{F}_i^f$:

$$\sum_{f=1}^{n_f}\left\{A_f(Q^2)\mathcal{F}_2^f, A_f(Q^2)\mathcal{F}_L^f, B_f(Q^2)\mathcal{F}_3^f\right\} = \{F_2/x, F_L/x, F_3\} \quad (22)$$

The total hadronic cross section is given by a convolution of the contributing parton subprocesses with their respective densities. An analogous decomposition holds for the structure functions. Up to and including the $O(\alpha_s)$ we have (see App. A):

$$\mathcal{F}_i^f = q_f^0 \otimes \mathcal{F}_i^q + \bar{q}_f^0 \otimes \mathcal{F}_i^{\bar{q}} + G^0 \otimes \mathcal{F}_i^G \qquad (i = 2, L, 3) \quad (23)$$

For $p = q, \bar{q}$ the $\mathcal{F}_i^p(x, Q^2, x_p)$ are the partonic structure functions initiated by a quark (antiquark) (of any flavour f) inside the proton, and $\mathcal{F}_i^G$ is the gluon initiated structure function yielding a quark-antiquark pair (of arbitrary flavour f). Note that we use the "bare" Q^2-independent parton densities q_f^0, $\bar{q}_f^0$ and G^0 in eq. (23). For convenience of writing we have introduced the notation

$$p \otimes f \equiv \int_x^1 \frac{dx_p}{x_p} p\left(\frac{x}{x_p}\right) f(x_p) \quad (24)$$

where p is the parton density and f is the parton cross section. Note that the lower bound in the x_p-integration is given by the scaling variable x. The partonic scaling variable x_p is related to η (the fraction of the proton's (longitudinal) momentum carried by the parton with momentum $p = \eta P$) via:

$$x_p = \frac{Q^2}{2pq} = \frac{x}{\eta} \quad (25)$$

In the naive QPM (i.e. at $O(\alpha_s^0)$) the "bare"parton densities are Q^2-independent and only the first two terms (quark and antiquark-initiated) in eq. (23) contribute. The inclusion of higher order QCD effects leads to evolving parton densities in eq. (23) (i.e. to redefined parton densities) as well as to fixed order higher order QCD contributions.

In order to be explicite we now list all terms that contribute to the partonic subprocesses up to $O(\alpha_s)$. The partonic structure functions $\mathcal{F}_i^p$ in eq. (23) can be readily obtained by suitable projections of the partonic tensor that describes the parton process initiated by a parton p. The appropiate projections can be obtained by using the n-dimensional covariants defined in eq. (A.9):

$$\mathcal{F}_2^p = \left(\frac{3-2\epsilon}{1-\epsilon}2x_p\frac{p^\mu p^\nu}{pq} - \frac{g^{\mu\nu}}{1-\epsilon}\right) W_{\mu\nu}^{(p)pc} \quad (26)$$

[2]Note that in n dimensions it is convenient to absorb a longitudinal contribution proportional to ϵy^2 in the definition of $\mathcal{F}_2$ in eq. (21) which, however, vanishes as $n \to 4$. Similarly, the factor $K(\epsilon)$, defined in eq. (A.6), goes to unity as $n \to 4$.

$$\mathcal{F}_L^p = 4(1-\epsilon)\,x_p\frac{p^\mu p^\nu}{pq}W_{\mu\nu}^{(p)pc}$$
$$\mathcal{F}_3^p = \frac{i}{pq}\epsilon^{\mu\nu\alpha\beta}q_\alpha p_\beta\, W_{\mu\nu}^{(p)pv}$$

Here the p.c. (p.v.) parton tensors $W_{\mu\nu}^{(p)pc/pv}$ are given by:

$$W_{\mu\nu}(p,q)^{(p)pc/pv} = \frac{1}{4\pi}\sum_N dPS^{(N)}H_{\mu\nu}^{(p)pc/pv}(p,q,p_1,\ldots,p_N) \quad (27)$$

where $H_{\mu\nu}^{(p)}(N)$ is the spin-averaged square of the N-body final-state amplitude contributing to the virtual-boson-parton p process $q + p \to p_1 + \ldots + p_N$ (excluding the electroweak couplings). $PS^{(N)}$ is the corresponding N-body Lorentz-invariant phase space. The details of the calculation are given in the appendices. There are some subtleties in calculating the p.v. structure function F_3 in the dimensional regularization scheme which are discussed in Appendix C. One obtains:

$$\mathcal{F}_2^q(x,x_p,Q^2) = \delta(1-x_p) + \frac{\alpha_s}{2\pi}\left(\left[\ln\frac{Q^2}{\mu^2} - \frac{1}{\epsilon'}\right]P_{qq}(x,x_p) + f_2^q(x,x_p)\right) \quad (28)$$
$$\mathcal{F}_L^q(x,x_p,Q^2) = \frac{\alpha_s}{2\pi}f_L^q(x_p)$$
$$\mathcal{F}_3^q(x,x_p,Q^2) = \delta(1-x_p) + \frac{\alpha_s}{2\pi}\left(\left[\ln\frac{Q^2}{\mu^2} - \frac{1}{\epsilon'}\right]P_{qq}(x,x_p) + f_3^q(x,x_p)\right)$$

$$\mathcal{F}_i^{\bar{q}}(x,x_p,Q^2) = \pm\mathcal{F}_i^q(x,x_p,Q^2) \qquad \begin{cases} i = 2, L \\ i = 3 \end{cases} \quad (29)$$

$$\mathcal{F}_2^G(x_p,Q^2) = \frac{\alpha_s}{2\pi}\left(\left[\ln\frac{Q^2}{\mu^2} - \frac{1}{\epsilon'}\right]P_{qG}(x_p) + f_2^G(x_p)\right) \quad (30)$$
$$\mathcal{F}_L^G(x_p,Q^2) = \frac{\alpha_s}{2\pi}f_L^G(x_p)$$
$$\mathcal{F}_3^G(x_p,Q^2) = 0$$

The Altarelli-Parisi (AP) kernels P_{qq}, P_{qG} and the finite $O(\alpha_s)$ contributions f_i^p are given in Appendix B. Note that P_{qq}, f_2^q and f_3^q do not only depend on x_p but also on x. The dependence on x comes in through the modified "+ distribution" (see eq.(B.24)) used to extract the δ-function singularity at $x_p = 1$. This brings in the lower limit x of the x_p integration of the convolution eq. (24). Thus the $x-$dependence can be viewed as an artifact of the modified "+ distribution" technique. Note that the modified AP kernel $P_{qq}(x,x_p)$ turns into the usual AP kernel $P_{qq}(x_p)$ when the lower integration limit is $x = 0$. μ in eqs. (28,30) is an arbitrary mass scale and ϵ' is defined by:

$$\frac{1}{\epsilon'} = \frac{1}{\epsilon} - \gamma + \ln 4\pi \quad (31)$$

where γ is the Euler constant.

Using eq.(23) we recover the QPM hadronic structure functions at the $O(\alpha_s^0)$:

$$\mathcal{F}_2^f(x,Q^2) = \mathcal{F}_2^f(x) = q_f^0(x) + \bar{q}_f^0(x) \quad (32)$$
$$\mathcal{F}_L^f(x,Q^2) = 0$$
$$\mathcal{F}_3^f(x,Q^2) = \mathcal{F}_3^p(x) = q_f^0(x) - \bar{q}_f^0(x)$$

In the QPM one has to use the "bare" mass scale independent parton distributions in eq. (32).

As mentioned before, initial state singularities (the $1/\epsilon$-terms) remain in eqs. (28,29, 30) and thus in the (hadronic) cross section via eqs. (23,21) even after adding real and virtual $O(\alpha_s)$ corrections. In order to absorb these singularities in the parton densities we need a prescription (a "scheme") how to "renormalize" the "bare" parton distributions $p_p^0(\eta)(\equiv q_f^0(\eta), \bar{q}_f^0(\eta), G^0(\eta))$. *One* possibility to define the parton densities beyond the leading order in QCD is given by the following requirement [AEM79]: The form of eq. (32) is preserved for the structure function $\mathcal{F}_2^f$ with no corrections proportional to α_s. To this end the "bare" parton densities $p_p^0(x)$ are to be replaced by the "renormalized" scale- (i.e. Q^2-) dependent parton distributions $p_p(x,Q^2)$. Thus one has [3]

$$\mathcal{F}_2^f(x,Q^2) = q_f(x,Q^2) + \bar{q}_f(x,Q^2) \tag{33}$$

This implies the following relationship between the bare and renormalised parton densities for the DIS to first order in α_s:

$$\begin{aligned} q_f(x,Q^2) = q_f^0(x) + \frac{\alpha_s}{2\pi}\int_x^1 \frac{dx_p}{x_p} \quad & \left\{ q_f(x/x_p,Q^2)\left(\left[\ln\frac{Q^2}{\mu^2} - \frac{1}{\epsilon}\right] P_{qq}(x,x_p) + f_2^q(x,x_p)\right) \right. \\ & \left. + \tfrac{1}{2}\, G(x/x_p,Q^2)\left(\left[\ln\frac{Q^2}{\mu^2} - \frac{1}{\epsilon}\right] P_{qG}(x_p) + f_2^G(x_p)\right)\right\} \end{aligned} \tag{34}$$

The antiquark distribution is obtained from eq. (34) by the relpacement $q \to \bar{q}$. The gluon distribution function is not renormalized in this order.

2.4 $O(\alpha_s)$ K-factor

Inserting eq. (34) and eqs. (28,29,30) in eq. (23) we obtain the (hadronic) structure functions up to $O(\alpha_s)$:

$$\begin{aligned} \mathcal{F}_2^f &= q_f + \bar{q}_f \\ \mathcal{F}_3^f &= (q_f - \bar{q}_f) + (q_f - \bar{q}_f) \otimes \frac{\alpha_s}{2\pi}\{f_3^q - f_2^q\} \\ \mathcal{F}_L^f &= (q_f + \bar{q}_f) \otimes \frac{\alpha_s}{2\pi} f_L^q + G \otimes \frac{\alpha_s}{2\pi} f_L^G \end{aligned} \tag{35}$$

In eq. (35) we have used the fact that $f_3^q = -f_3^q$ and $f_3^G = 0$. The explicit forms of the $O(\alpha_s)$ correction terms are given by ($C_F = 4/3$ and $T_R = 1/2$):

$$\begin{aligned} f_L^q(x_p) &= C_F\, 2x_p \\ f_L^G(x_p) &= T_R\, 8x_p(1-x_p) \\ f_3^q(x_p) - f_2^q(x_p) &= -C_F(1+x_p) \end{aligned} \tag{36}$$

After reinserting the heavy flavour contributions we obtain the following expressions for the current structure functions from eq. (19):

$$F_2(x,Q^2) = x\sum_{f=1}^{n_f} A_f(Q^2)\left[q_f(x,Q^2) + \bar{q}_f(x,Q^2)\right] + \frac{\alpha_s}{2\pi} F_2[HF](x,Q^2) \tag{37}$$

[3] Note that this definition implies that $\mathcal{F}_2^f[\mathrm{NLL}](x,Q^2) = \mathcal{F}_2^f[\mathrm{LL}](x,Q^2)$.

$$\begin{aligned} F_L(x,Q^2) &= x\frac{\alpha_s}{2\pi}\sum_{f=1}^{n_f} A_f(Q^2)\int_x^1 \frac{dx_p}{x_p}\left\{\left[q_f(x/x_p,Q^2) + \bar{q}_f(x/x_p,Q^2)\right] C_F\, 2x_p \right. \\ &\quad \left. + G(x/x_p,Q^2) T_R\, 8x_p(1-x_p)\right\} + \frac{\alpha_s}{2\pi} F_L[HF](x,Q^2) \\ F_3(x,Q^2) &= \sum_{f=1}^{n_f} B_f(Q^2)\left[q_f(x,Q^2) - \bar{q}_f(x,Q^2)\right] \\ &\quad - \frac{\alpha_s}{2\pi}\sum_{f=1}^{n_f} B_f(Q^2)\int_x^1 \frac{dx_p}{x_p}\left[q_f(x/x_p,Q^2) - \bar{q}_f(x/x_p,Q^2)\right] C_F(1+x_p) \\ &\quad + \frac{\alpha_s}{2\pi} F_3[HF](x,Q^2) \end{aligned}$$

An alternative way of expressing the longitudinal structure function is:

$$F_L(x,Q^2) = C_F\frac{\alpha_s}{\pi}\int_x^1 \frac{d\eta}{\eta}\left(\frac{x}{\eta}\right)^2\left\{F_2(\eta,Q^2) + \left(\sum_{f=1}^{n_f} A_f(Q^2)\right)\frac{4T_R}{C_F}\left(1-\frac{x}{\eta}\right)\eta G(\eta,Q^2)\right\} \tag{38}$$

We recover the well known result for F_L [AM78] when taking four light flavours in the pure photon exchange limit where $4T_R/C_F\sum_f A_f^2 = 5/3$. The expressions for the heavy flavour structure functions appearing in eq. (37) can be found e.g. in [Sch87]. We will neglect their contribution in the following.[4]

Using the above expressions for the DIS structure functions in eq. (18) we obtain the total $O(\alpha_s)$ corrected e^-p cross section in the NC case.

Before we present the result for the $O(\alpha_s)$ NC K-factor as defined in eq.(20) we first derive the $O(\alpha_s)$ corrected cross section formula for charged current events in e^-p scattering. Again, ρ is the lepton longitudinal polarization ($\rho = 0$ for unpolarized leptons, $\rho = 1(-1)$ for right-handed (left-handed) leptons). We introduce the abbreviations N_u, N_d, n_u and n_d. For e^-p-scattering N_u (N_d) gives the maximum number of up-like quarks (down-like antiquarks) within the proton which can participate the reaction, whereas in e^+p collisions N_u (N_d) gives the maximum number of up-like antiquarks (down-like quarks) within the proton. Similarly, for e^-p- (e^+p-) scattering, n_u and n_d give the maximum number of up-like antiquarks and down-like quarks (up-like quarks and down-like antiquarks) which can be produced in antiquark and quark (quark and antiquark) initiated reactions, respectively. n_u and n_d also count the maximum number of up-like antiquarks and down-like quarks (up-like quarks and down-like antiquarks) which can be produced in boson-gluon fusion in e^-p- (e^+p-) scattering, respectively. The actual values of n_u and n_d depend on the available hadronic energy W. If W is above the threshold of a given quark pair creation process the latter will be included. For e^-p-scattering we then find (m_W is the W-boson mass and $V_{ff'}$ denote the Kobayashi-Maskawa matrix elements):

$$\begin{aligned} \frac{1}{xs}\frac{d^2\sigma(e^-p)}{dxdy} &= \frac{(1-\rho)\pi\alpha^2}{4\sin^4\theta_W(Q^2+m_W^2)^2}\left\{\sum_{f=u}^{N_u} q_f(x,Q^2)\sum_{f'=d}^{n_d} \mid V_{ff'}\mid^2 \right. \\ &\quad \left. + (1-y)^2\sum_{f=d}^{N_d}\bar{q}_f(x,Q^2)\sum_{f'=u}^{n_u}\mid V_{f'f}\mid^2 + \frac{\alpha_s}{4\pi}\int_x^1\frac{dx_p}{x_p}C^-(x,x_p,Q^2)\right\} \end{aligned} \tag{39}$$

[4] In the true deep inelastic region ($Q^2 \geq 5\,\mathrm{GeV}^2$) their contribution to the NC cross section is very small since NC heavy flavour production proceeds essentially by photoproduction. In the CC case, heavy flavour production (as e.g. tb) is a negligible contribution to the total CC cross section if one treats the charmed quark as massless.

The $O(\alpha_s)$ correction factor C^- in eq.(39) is given by:

$$\begin{aligned} C^-(x,x_p,Q^2) &= -y^2 G(x/x_p,Q^2)\, f_L^G(x_p) \left[\sum_{f=u}^{n_u}\sum_{f'=d}^{n_d} \mid V_{ff'} \mid^2\right] \\ &+ \sum_{f=u}^{N_u} q_f(x/x_p,Q^2)\left[-y^2 f_L^q(x_p) + Y_-\left(f_3^q(x_p) - f_2^q(x_p)\right)\right] \sum_{f'=d}^{n_d} \mid V_{ff'} \mid^2 \\ &+ \sum_{f=d}^{N_d} \bar{q}_f(x/x_p,Q^2)\left[-y^2 f_L^q(x_p) - Y_-\left(f_3^q(x_p) - f_2^q(x_p)\right)\right] \sum_{f'=u}^{n_u} \mid V_{f'f} \mid^2 \end{aligned} \tag{40}$$

The corresponding e^+p cross section formula are obtained from eq. (39) by the interchange of the quark and antiquark densities and $\rho \leftrightarrow -\rho$ as implied by eqs.(12, 15).

For the actual calculation we have assumed the top mass to be sufficient heavy so that $m_b < W < m_t$. Then, by using:

$$\sum_{f=u}^{N_u} = \sum_{f=u,c}; \quad \sum_{f=d}^{N_d} = \sum_{f=d,s}; \quad \sum_{f=u}^{n_u} = \sum_{f=u,c}; \quad \sum_{f=d}^{n_d} = \sum_{f=d,s,b} \tag{41}$$

and the unitarity relations of the KM-matrix, the e^-p cross section simplifies to:

$$\begin{aligned} \frac{1}{xs}\frac{d^2\sigma(e^-p)}{dxdy} &= \frac{(1-\rho)\pi\alpha^2}{4\sin^4\theta_W(Q^2+m_W^2)^2}\left\{\left[u(x,Q^2)+c(x,Q^2)\right]\right. \\ &+(1-y)^2\left[\left(1-\mid V_{td}\mid^2\right)\bar{d}(x,Q^2)+\left(1-\mid V_{ts}\mid^2\right)\bar{s}(x,Q^2)\right] \\ &\left.+\frac{\alpha_s}{4\pi}\int_x^1\frac{dx_p}{x_p}C^-(x,Q^2,x_p)\right\} \end{aligned} \tag{42}$$

where now:

$$\begin{aligned} C^-(x,Q^2,x_p) &= -2y^2 G(x/x_p,Q^2)\, f_L^G(x_p) \\ &+\left[u(x/x_p,Q^2)+c(x/x_p,Q^2)\right]\left[-y^2 f_L^q(x_p)+Y_-\left(f_3^q(x_p)-f_2^q(x_p)\right)\right] \\ &+\left[\left(1-\mid V_{td}\mid^2\right)\bar{d}(x/x_p,Q^2)+\left(1-\mid V_{ts}\mid^2\right)\bar{s}(x/x_p,Q^2)\right] \\ &\times\left[-y^2 f_L^q(x_p)-Y_-\left(f_3^q(x_p)-f_2^q(x_p)\right)\right] \end{aligned} \tag{43}$$

Here u stands for the u-quark density etc. Note finally that:

$$\frac{\pi\alpha^2}{4\sin^4\theta_W(Q^2+m_W^2)^2} = \frac{G_F^2(1-\Delta r)^2}{2\pi}\left(1+\frac{Q^2}{m_W^2}\right)^{-2} \tag{44}$$

where G_F is the Fermi coupling constant and Δr is an electro-weak correction factor ($\Delta r = 0.0696$).

We now present results for the $O(\alpha_s)$ K-factor eq. (20) at the nominal HERA cms energy $\sqrt{s} = 314\,\mathrm{GeV}$ both in NC and the CC case. For the calculation we use the one-loop expression of $\alpha_s(M_\alpha^2)$ with five flavours and $\Lambda_{QCD} = 0.2\,\mathrm{GeV}$. M_α is the mass scale of the running coupling constant α_s. The parton density parametrization is from [GHR82] which allows for three flavours (u,d,s) within the proton. Thus the charm density appearing in the eqs.(41, 42, 43) is effectively set to zero. We allow four (NC) and five (CC)flavours to

be produced in the boson-gluon fusion process. The other parameters are $\sin^2\theta_W = 0.217$, $m_W = 81.8\,GeV$, $m_Z = 93.8\,GeV$, $\alpha = 1/137$, V_{td}=V_{ts}=0. We emphasize again that the K-factor does depend on the scheme used to redefine the parton densities. In addition, K depends also on the mass scale M_α and on the mass scale M_p used in the parametrization of the parton densities [5]. Since Q is chosen as mass scale in the parametrizations of the parton distribution functions ($M_p = Q$) we have to set $M_\alpha = M_p = Q$.

The resulting K-factors for the NC and CC case are shown in Fig. 2 a,b as a function of Q^2 for various values of x. The respective curves terminate at the kinematic limits $Q^2 < xs$ given by the nominal HERA CM energy $\sqrt{s} = 314$GeV. We find that $K(x,Q^2)$ is always smaller than one as the NLL terms coming fron F_L and F_3 contribute negatively to the NC and CC cross sections (see eqs. 18,37,39,40). For $x \geq 0.1$ the K-factor is approximately one over the whole Q^2 range (the maximal deviation from unity is less than 4 %). Therefore one can use the LL DIS structure functions for $x \geq 0.1$ without incurring too large of an error.

We find that $K(x,Q^2)$ deviates substantially from unity for x decreasing below $\cong 0.1$. The deviation increases for increasing Q^2. This behaviour has its origin in the important contribution of the gluon density to the K-factor. The dominance of the gluon density for small x is even amplified due to the Q^2 evolution for increasing Q^2. A second reason for the variation of the K-factors with Q^2 is that the variable y tends to one with increasing Q^2 for fixed values of x due to the relation $Q^2 = xys$. The ratios of the y-dependent factors in front of F_3 and F_L on the one hand and the y-dependent factor in front of F_2 on the other hand, i.e. Y_-/Y_+ and $(-y^2)/Y_+$ become maximal in the limit $y \to 1$ (see eq. (18)) thus enhancing the NLL contributions of F_3 and F_L. This means that the effects of the K-factors can no longer be neglected for very small x. On the one hand, the overall rate is substantially diminished and, on the other hand, the distributions in the kinematical variables (x,Q^2) or (x,y) is changed. Thus these variables can no longer be generated according to the LL formula eq.(10) in this kinematic range in e.g. explicit Monte Carlo generators as in [IN87]. In particular the W-distribution ($W^2 = (1-x)Q^2/x$) becomes softer. This has consequences for the predicted jet multiplicity in leptoproduction (see eq.(64)). When the K-factors deviate from unity by a large amount the usual Altarelli-Parisi evolution based on the LL approximation becomes questionable and reliable predictions can no longer be made. Such a situation occurs for x smaller than $10^{-2} - 10^{-3}$ depending on Q^2 (see figs. 2a and 2b). HERA with its large nominal CM energy $\sqrt{s} = 314$ GeV will afford an opportunity to explore this very interesting low x-region. From figs. 2a and 2b one sees, however, that the Q^2-range where $|K-1|$ is large (> 0.15) is quite small for a given and fixed small x which makes such an exploration difficult. Also note that theoretical predictions for the totally integrated cross section are not much affected by these contributions.

[5] The mass scale M_p is sometimes also referred to as the factorization mass.

3 Jet cross sections in $O(\alpha_s)$

The QPM ($O(\alpha_s^0)$) processes (4) predict two and only two jets in the final state, namely the struck quark jet and the proton remnant jet. The $O(\alpha_s)$ tree graph processes (16) give rise to 3-jet production (Fig. 1e). One jet originates from the proton remnant, a second jet from the struck quark and the third jet is due to hard gluon radiation (or due to boson-gluon fusion into a well separated quark-antiquark pair). There are singular regions in the phase space of the $O(\alpha_s)$ tree graph cross section (hereafter referred to as the 3-parton phase space). These singular contributions correspond physically to the situation where two (or more) partons are irresolvable and have to be counted as contribution to the 2-jet cross section. Parts of these singular cross section contributions will cancel against corresponding singular terms of the $O(\alpha_s)$ virtual 2-parton corrections. In contrast to the e^+e^- case, the cancellation is only partial and singular terms remain. As mentioned before they originate from initial state mass singularities, which have to absorbed by a suitable redefinition of the parton densities. We shall comment on the differences of the parton branching probabilities in leptoproduction and e^+e^--production. We then come to the question, what is the probability, R_2, that an event will be 2-jet (3-jet) like for a given kinematical configuration specified by (x, Q^2).

3.1 3-jet cross section

While the $O(\alpha_s^0)$ 2-jet cross section, i.e. the QPM processes (4) are desribed by two independent kinematical variables, e.g. x and y, the $O(\alpha_s)$ tree graph processes (16) possess a richer kinematical structure. Not only is the dependence on the two variables x and y modified but in addition three more variables are needed to describe the reactions (16). In addition to x_p (which is trivial in the 2-parton case) we choose the scaling variable z defined by

$$z = \frac{p \cdot p_1}{p \cdot q} \tag{45}$$

and Φ, the azimuthal angle between the parton plane $(\vec{p}, \vec{p}_1)$ and the lepton plane $(\vec{l}, \vec{l}')$ in the cms $\vec{p} + \vec{q} = 0$.

Analogous to the e^+e^- case we find it convenient to introduce helicity cross sections $d\sigma_\alpha$ which correspond to certain polarization states of the exchanged virtual boson. To $O(\alpha_s)$ one has 4 p.c. independent helicity cross section which are labelled by $\alpha = U + L, L, T, I$ and two p.v. helicity cross sections $\alpha = P, A$. In order to obtain the genuine 3-jet cross sections it is clear that we only need the 4-dimensional parts of the helicity cross sections given in App. C. The expressions for the 3-jet cross sections agree with those of [Me78, FP82, PR80] expect for a minus sign misprint in [PR80].

As in the case of the QPM cross section eq. (10) the electro-weak dependence of the helicity cross sections is determined by their p.c. or p.v. character, respectively: The p.c. cross sections are governed by $A_f(Q^2)$ whereas the p.v. cross sections are governed by $B_f(Q^2)$. Furthermore, each of the helicity cross sections carries a definite y and Φ dependence which is specified by the coefficients $g_\alpha(y, \Phi)$ given in eq. (B.19). For the NC e^-p scattering case we obtain the $O(\alpha_s)$ tree graph cross section [Me78, PR80, FP82]:

$$\frac{2\pi x_p\, d^5\sigma}{dx dy dx_p dz d\Phi} = \frac{2\pi\alpha^2}{yQ^2}\,\frac{\alpha_s}{2\pi}\,\{I_G + I_q\} \tag{46}$$

I_G denotes the gluon-initiated contribution:

$$I_G = G(x/x_p, Q^2)\left\{\left(\sum_{f=1}^{N_f} A_f(Q^2)\right)\sum_{\alpha=U+L,L,T,I} g_\alpha(y,\Phi)\frac{d^2\sigma_G^\alpha}{dx_p dz} + \left(\sum_{f=1}^{N_f} B_f(Q^2)\right)\sum_{\alpha=P,A} g_\alpha(y,\Phi)\frac{d^2\sigma_G^\alpha}{dx_p dz}\right\} \tag{47}$$

and I_q gives the quark- and antiquark-initiated contributions:

$$I_q = \sum_{f=1}^{n_f}\left\{\left[q_f(x/x_p, Q^2) + \bar{q}_f(x/x_p, Q^2)\right] A_f(Q^2)\left(\sum_{\alpha=U+L,L,T,I} g_\alpha(y,\Phi)\frac{d^2\sigma_q^\alpha}{dx_p dz}\right) + \left[q_f(x/x_p, Q^2) - \bar{q}_f(x/x_p, Q^2)\right] B_f(Q^2)\left(\sum_{\alpha=P,A} g_\alpha(y,\Phi)\frac{d^2\sigma_q^\alpha}{dx_p dz}\right)\right\} \tag{48}$$

3.2 Jet measures

As was mentioned before, the $O(\alpha_s)$ tree graph cross section as given in eq. (46) becomes singular in certain regions of the (3-parton) phase space. For the quark-initiated process (16) we denote the momentum of the initial (final) state quark by p (p_1) and the gluon momentum by p_2. Then its singularity structure is exhibited by (see App. C).

$$d\sigma^q \propto \frac{4[(pq - p_1p_2)^2(pp_1)^2 + (pq)^4]}{2pp_2\, 2p_1p_2\, (pq)^2} = \frac{1 + x_p^2z^2}{(1-z)(1-x_p)} \tag{49}$$

We find that $d\sigma^q$ diverges for the following kinematic configurations:

p_2 collinear to p	$\Rightarrow$	$z \to 1$
p_2 collinear to p_1	$\Rightarrow$	$x_p \to 1$
p_2 soft	$\Rightarrow$	$z, x_p \to 1$

(Collinear singularities are also called mass singularities, whereas soft singularities are referred to as infrared ones.) Similarly, in the gluon-initiated process of (16), we denote the momentum of the (initial state) gluon by p and the quark (antiquark) momentum of the final state by $p_1(p_2)$. Its singularity structure is given by:

$$d\sigma^G \propto \frac{4[(pp_1)^2 + (pp_2)^2][(pq - p_1p_2)^2 + (p_1p_2)^2]}{2pp_1\, 2pp_2\, (pq)^2} = \frac{[z^2 + (1-z)^2][x_p^2 + (1-x_p^2]}{z(1-z)} \tag{50}$$

Here the cross section $d\sigma^G$ diverges if

p_2 collinear to p	$\Rightarrow$	$z \to 1$
p_1 collinear to p	$\Rightarrow$	$z \to 0$
p_2 soft	$\Rightarrow$	$z \to 1$
p_1 soft	$\Rightarrow$	$z \to 0$

Clearly, in the singular regions one no longer has well separated partons that can fragment into clearly distinguished jets. A jet criterium has to be introduced in order to define a genuine 3-jet region in the 3-parton phase space.

It is clear that Sterman-Weinberg like energy-angle cuts are not a good choice to define the 3-jet region. Contrary to the e^+e^--case, the hadronic CMS and the Lab-system do not coincide in leptoproduction. The typical large boosts that have to be applied along the proton axis in order to get from the CMS to the Lab-system will influence the widths, separations and energies of the jets (see [BIR87]). Two jets that are resolved by an energy-angle cut in one system become irresolvable in the other system. It is clear that one has to define resolvability (and thereby the 3-jet region) by using invariant mass-cuts.

Let us first recall that the 3-parton phase space is described by the three variables x_p, z and the azimuthal angle Φ besides x and y which are taken to be fixed for the present discussions. The azimuthal variable has no bearing on the jet definition.

Let us now delineate the 3 parton phase space. The total phase space is given by:
total phase space

$$x \leq x_p \leq 1 \quad ; \quad 0 \leq z \leq 1 \tag{51}$$

The genuine 3-jet region, to be defined by a suitable invariant mass jet criterium, clearly should exclude the singularities at $z = 0, 1$ and $x_p = 1$. Its general form can be written as:
3-jet region

$$\begin{aligned} z_{min} \leq z \leq z_{max} \\ x_{p,min} \leq x_p \leq x_{p,max} \end{aligned} \tag{52}$$

It is clear that the 3-jet cross section will depend on the specific way in which the 3-jet region eq. (52) is set up.
Before examing the more complicated ep-case let us first recall some facts of jet definition in e^+e^- interactions. Two partons i and j are said to be irresolvable if their squared invariant mass s_{ij} satisfies:

$$s_{ij} \equiv (p_i + p_j)^2 \leq y_{cut} s \tag{53}$$

p_i, p_j are the particle momenta, s is the (constant) cms energy and y_{cut} the (constant) cut-off parameter. One then *defines*: A 3-parton final state (with momenta p_1, p_2 and p_3) counts as 2-jet event if *any* of the three squared invariant masses is smaller than y_{cut} times s. Or vice versa: To be a (genuine) 3-jet event, all scaled invariant masses $y_{ij} \equiv s_{ij}/s$ of the 3-parton event must be bigger than the cut-off y_{cut}:

$$d\sigma[3-jet] = \prod_{i \neq j} \Theta(y_{ij} - y_{cut}) d\sigma[3-parton] \tag{54}$$

Complementary, the real (tree graph) contribution to the 2-jet cross section is arrived at by integrating the 3-parton cross section over the unresolved regions of the 3-particle phase space (i.e. over the phase space complement as it occurs in eq. (54)). Note that this definition of 2- (3-) jet-likeness corresponds to the so called direct dressing scheme. We mention finally that the irresolvability criterium eq. (53) can fully be expressed by the final parton momenta via $s \equiv (p_{e^-} + p_{e^+})^2 = (p_1 + p_2 + p_3)^2$ and that the analysis is most conviently done in the final hadronic cms $\vec{p_1} + \vec{p_2} + \vec{p_3} = 0$.

Let us now turn to the case of deep inelastic scattering and attempt to define invariant mass jet resolution criteria. One would like to remain as close as possible to the e^+e^- example. Thus a "natural" choice for analysing jets is the final hadronic cms $\vec{P} + \vec{q} = 0 = \vec{p_1} + \vec{p_2} + \vec{p_3}$ and to use the hadronic mass W^2 eq. (3) as reference mass[6]. The 3-jet-likeness

[6]Remember that p_3 is the momentum of the proton remnants, see Fig. 1e.

criterium analogous to the e^+e^--case eq. (54) is:

$$s_{ij} \geq y_{cut} W^2 \equiv y_{cut}(p_1 + p_2 + p_3)^2 \quad , \quad (i \neq j = 1, 2, 3) \tag{55}$$

In the following we shall refer to the jet definition scheme eq. (55) as the "W-scheme". In terms of the integration variables z and x_p the corresponding 3-jet region is given by eq. (52) with the following upper and lower integration limits [7]:
W-scheme

$$\begin{aligned} z_{min} &= \frac{(1-x)x_p}{x_p - x} y_{cut} = 1 - z_{max} \\ x_{p,min} &= \frac{x}{1 - 2(1-x)y_{cut}} \\ x_{p,max} &= \frac{x}{x + (1-x)y_{cut}} \end{aligned} \tag{56}$$

A different jet definition scheme is arrived at by noting that there are two mass scales in DIS, namely W^2 and Q^2. For consistency reasons it would be desirable to use the same mass scale in the jet definition, in the running coupling constant α_s and in the parton densities. Since the usual mass scale in DIS is Q^2 this would then lead us to the "Q-scheme" where the resolvability is defined by:

$$s_{ij} \geq y_{cut} Q^2 \quad , \quad (i \neq j = 1, 2, 3) \tag{57}$$

The z and x_p integration limits of the corresponding 3-jet region are given by:
Q-scheme

$$\begin{aligned} z_{min} &= \frac{x x_p}{x_p - x} y_{cut} = 1 - z_{max} \\ x_{p,min} &= \frac{x}{1 - 2x y_{cut}} \\ x_{p,max} &= \frac{1}{1 + y_{cut}} \end{aligned} \tag{58}$$

Yet another jet criterium is arrived at by requiring that the two dimensional integrations of the 3-parton phase space decouple in the sense that the z integration limits do not depend on x_p. We shall refer to this jet definition scheme as the "mixed" scheme as both W^2 and Q^2 appear as mass scales in this scheme.
mixed scheme

$$\begin{aligned} z_{min} &= y_{cut} = 1 - z_{max} \\ x_{p,min} &= x \\ x_{p,max} &= \max(1 - y_{cut}, x) \end{aligned} \tag{59}$$

One notes that the mixed scheme 3-jet region does not depend on the "outer" variables x and Q^2. When expressed in terms of invariants the mixed scheme 3-jet criteria read:

$$\begin{aligned} &(i) \quad 2p_1 \cdot p_2 \geq \frac{y_{cut}}{1 - y_{cut}} Q^2 \\ &(ii) \quad 2p_1 \cdot P \geq y_{cut}(W^2 + Q^2) \\ &(iii) \quad 2p_2 \cdot P \geq y_{cut}(W^2 + Q^2) \end{aligned} \tag{60}$$

[7]The integration limits agree with the results of In86.

It is important to note that the proton momentum P is used in eq. (60) instead of the momentum p_3 of the proton remnant jet as is done in the W- and Q-scheme.

We also observe that the jet definition criterium, given either by eq. (55), eq. (57) or eq. (60), is x and y dependent. For every given pair (x,y) (or (x,Q^2)) we actually choose a *different* effective cut-off y_{cut}, i.e. the allowed range for the invariant masses becomes (x,Q^2)-dependent. Take for example the Lab-system where the total cms energy is the only fixed reference mass available. Eq. (55) must be read as:

$$s_{ij} \geq y_{cut}(1-x)ys \equiv y_{cut,eff}(x,y)\, s \tag{61}$$

In order to obtain a fixed three jet fraction for any given hadronic energy W (e.g. the fraction measured for that energy in e^+e^- collisions), one has to adjust the cut parameter y_{cut}, i.e. make it varying.

The 3-jet phase space regions defined according to the three 3-jetdefinition schemes are shown in Fig. 3. Since these regions are x-dependent they are given for two different values of x namely $x = 0.5$ and $x = 0.1$.

Let us first start with the mixed scheme in Fig 3c since it has the simplest 3-jet phase space boundaries. The 3-jet region becomes smaller as x increases but the distance from the singularities at $z = 0,1$ and $x_p = 1$ remains constant. This differs from what we find for the W-scheme in Fig. 3a where W defines the mass scale eq. (56): The distance from the $z = 0,1$ singularities is still x-independent, but the smaller the 3-region becomes (with increasing x) the closer we come to the $x_p = 1$ singularity, i.e. the more of the phase space region close to the initial state "singularity" at $x_p = 1$ will be included in the 3-jet cross section. We thus expect a compensation effect in this case resulting in a less x-dependent 3-jet cross section. The 3-jet phase space boundaries of the Q-scheme are shown in Fig. 3b. One observes that one gets closer to the singulaities at $z = 0$ and $z = 1$ when the phase space becomes larger.

Finally we note that there is an additional sublety in defining jets in ep-collisions: the above procedure does *not* isolate the quark and gluon jets from their production origins, in contrast to the fragmentation picture in the e^+e^- case: In e^+e^- interactions, final state radiation is the only source of jet production, whereas in ep collisions, final and initial state radiation is possible. Obviously, in ep collisions, the probability for a gluon to come from the branching of a quark within the proton is proportional to the respective quark density, whereas the probability for a quark produced in e^+e^- reaction to branch is independent of this density. Thus, while the latter probability is (essentially) governed by the Altarelli-Parisi (AP) splitting kernels, the former probability contains in addition the respective parton density p. For example, in the limit of collinear emission the branching probability is a product of an AP kernel and the ratio $p(\eta,Q^2)/p(x,Q^2)$, where η is the momentum fraction of the proton carried by the parton: (see eq. (49) and (71)).

$$\text{branching probability} \sim \frac{d\hat{t}}{\hat{t}}\frac{dx_p}{x_p}\frac{p_q(x/x_p,Q^2)}{p_q(x,Q^2)}P_{qq}(x_p) \tag{62}$$

where $\hat{t} = (p_q - p_g)^2$ ($\hat{t}$ is spacelike!) (see also [BSZ86]). If initial and final state radiation were separate, the parton densities would appear only in the case of initial state radiation. It is the interference terms that also make final state radiation depend on a factor containing the ratio of parton densities evaluated at $\eta := x(1+m^2/Q^2)$ and at x

($m^2 = (p_q + p_g)^2$ is the off-shellness of the mother parton):

$$\text{branching probability} \sim \frac{dm^2}{m^2}\frac{p_q(x(1+m^2/Q^2),Q^2)}{p_q(x,Q^2)}P_{qq}(z)dz \tag{63}$$

The factor $p_q(\eta,Q^2)/p_q(x,Q^2)$ in eq. (62) in turn causes a reduction of final state radiation in leptoproduction as compared to the case where final state radiation could be treated independently. In passing we note that assuming the separation of initial and final state radiation and considering the limit of collinear emission, where the respective branching probabilities become process and flavour independent, it is possible to realize iterative parton branchings via a parton shower approach (for more details see [BSZ86]). Yet we emphasize that our full $O(\alpha_s)$ calculation insures a 3-jet rate that takes proper care of both the interference terms and its complete electro-weak dependence. We conclude that jet-likeness in e^+e^- reactions can be defined purely on the parton level, whereas the jet rates and widths in ep collisions are determined by the specific hadronic and leptoproduction origin of the partons. In the next section we will show the final behaviour of the 3-jet cross section for the various jet definition schemes taking into account the respective partonic cross sections and the (different ranges of) integration over the parton densities.

3.3 The $O(\alpha_s)$ Jet Ratios

We are now in the position to calculate the $O(\alpha_s)$ 2- and 3-jet jet ratios. We define the 3-jet rate $R_3(x,y)$ by:

$$\frac{d^2\sigma}{dxdy}[\text{3-jet}] = R_3(x,y)\frac{d^2\sigma}{dxdy}[\text{total}\,\alpha_s] \tag{64}$$

The $O(\alpha_s)$ 2-jet ratio R_2 is defined accordingly. Note that the 2- and 3-jet ratios are normalized to the $O(\alpha_s)$ corrected total cross section so that [8]

$$R_2(x,y) + R_3(x,y) = 1 \tag{65}$$

Let us first discuss the 2-jet ratio R_2. The calculation of R_2 consists of three steps: (i) The n-dimensional (partonic) tree graph cross sections of $O(\alpha_s)$ have to be integrated over the singular 2-jet region; (ii) one then adds on the $O(\alpha_s^0)$ Born term and the virtual $O(\alpha_s)$ corrections; (iii) the parton densities have to redefined in order to absorb the remaining initial state mass singularity (possibly together with certain finite pieces). A simpler way to obtain R_2 is by the difference $R_2(x,y) = 1 - R_3(x,y)$. Calculating R_2 this way has two advantages. Firstly, we can use the simpler 4-dimensional partonic cross section expressions to calculate R_3 since they are integrated over the finite 3-jet region of the 3-parton phase space. Secondly, for the genuine 3-jet cross section we do not have to redefine the parton densities in $O(\alpha_s)$ since the 3-parton cross section start at this order. Note though that R_3 depends on this redefinition through its dependence on the total $O(\alpha_s)$ cross section in the denominator of eq.(64).[9]

[8] This extends the calculation of $R_{2,3}$ in [S150, In87] where the total cross section in eq. (64) was approximated by the Born cross section.

[9] We have in fact gone through the instructive exercise of checking that the answer of both the above methods to calculate $R_2(x,y)$ agree. We stress that latter "trick" is not available to short-cut the calculation of the $O(\alpha_s^2)$ corrections to the 3-jet cross section.

The differential $O(\alpha_s)$ cross section necessary to calculate $R_3(x,y)$ in eq. (64) has already be given in section 2. The total $O(\alpha_s)$ 3-jet cross section is obtained by integrating over the 3-jet phase space:

$$\frac{d^2\sigma}{dxdy}[\text{3-jet}] = \frac{2\pi\alpha^2}{yQ^2}\frac{\alpha_s}{2\pi}\int_{x_{p,min}}^{x_{p,max}}\frac{dx_p}{x_p}\int_{z_{min}}^{z_{max}}dz\int_0^{2\pi}\frac{d\Phi}{2\pi}\{I_G+I_q\} \tag{66}$$

where the 3-jet intgrands I_G and I_q are given in eqs. (47,48). The integration limits for our three jet definition schemes are detailed in eqs. (56,58,59).

The Φ-integration can be done with ease. It implies an azimuthal averaging which eliminates the contributions of the helicity cross sections $d\sigma_\alpha$ with $\alpha = T, I, A$ in eq.(66) The z- and x_p-integration of $d\sigma_{U+L}$, $d\sigma_L$ and $d\sigma_P$ results in the 3-jet structure functions $\mathcal{F}_2$[3-jet], $\mathcal{F}_L$[3-jet] and $\mathcal{F}_3$[3-jet], respectively. One obtains:

$$\begin{aligned}\frac{d^2\sigma}{dxdy}[\text{3-jet}] &= \frac{2\pi\alpha^2}{Q^2y}\sum_{f=1}^{n_f}\Big[A_f(Q^2)\left\{Y_+\mathcal{F}_2^f[\text{3-jet}](x,Q^2)-y^2\mathcal{F}_L^f[\text{3-jet}](x,Q^2)\right\} \\ &\quad + B_f(Q^2)\,Y_-\,\mathcal{F}_3^f[\text{3-jet}](x,Q^2)\Big]\end{aligned} \tag{67}$$

where:

$$\begin{aligned}\mathcal{F}^f_{2,L,3}[\text{3-jet}]\ (x,y) &= \frac{\alpha_s}{2\pi}\int_{x_{p,min}}^{x_{p,max}}\frac{dx_p}{x_p}\int_{z_{min}}^{z_{max}}dz \\ &\quad \left\{\left[q_f(x/x_p,Q^2)\pm\bar{q}_f(x/x_p,Q^2)\right]\frac{d^2\sigma_q^{U+L,L,P}}{dx_pdz}+G(x/x_p,Q^2)\frac{d^2\sigma_G^{U+L,L,P}}{dx_pdz}\right\}\end{aligned} \tag{68}$$

Here the "+" sign obtains for the index $i = 2, L$ and the "−" sign for the index 3 of $\mathcal{F}^f$. The z-integration can be done in a straightforward way and one obtains[10]:

$$\begin{aligned}\int_{z_{min}}^{z_{max}}dz\,\frac{d^2\sigma_2^q}{dx_pdz} &= \frac{C_F}{1-x_p}\left\{-(1+x_p)^2\ln\frac{z_{min}}{1-z_{min}}+\frac{1}{2}(1-2z_{min})(1+2x_p-6x_p^2)\right\} \\ \int_{z_{min}}^{z_{max}}dz\,\frac{d^2\sigma_L^q}{dx_pdz} &= C_F\,2x_p(1-2z_{min}) \\ \int_{z_{min}}^{z_{max}}dz\,\frac{d^2\sigma_3^q}{dx_pdz} &= -C_F\,(1-2z_{min})(1+x_p)+\int_{z_{min}}^{z_{max}}dz\,\frac{d^2\sigma_2^q}{dx_pdz}\end{aligned} \tag{69}$$

and:

$$\begin{aligned}\int_{z_{min}}^{z_{max}}dz\,\frac{d^2\sigma_2^G}{dx_pdz} &= 2T_R\left\{[-1+6x_p(1-x_p)](1-2z_{min})-[1-2x_p(1-x_p)]\ln\frac{z_{min}}{1-z_{min}}\right\} \\ \int_{z_{min}}^{z_{max}}dz\,\frac{d^2\sigma_L^G}{dx_pdz} &= 2T_R\,4x_p(1-x_p)(1-2z_{min}) \\ \int_{z_{min}}^{z_{max}}dz\,\frac{d^2\sigma_3^G}{dx_pdz} &= 0\end{aligned} \tag{70}$$

The x_p-integration in eq. (68) has to be done numerically since it involves the integration over the parton densities. For our numerical results below we take the invariant mass cut-off parameter to be $y_{cut} = 0.04$. All other parameteres are as quoted in subsection 2.4.

[10] We agree with the unpublished result of [In86]. Note that $d\sigma_2$ in the subroutine QCDI of [In86] corresponds to $d\sigma_U$ in our notation.

The result of our calculation of the 3-jet rate is shown in Figs. 4-6. We do not show the 2-jet rate explicitly since it is simply given by $R_2(x,y,) = 1 - R_3(x,y)$. We plot the values of the 3-jet ratios R_3 as a function of x and Q^2 for each of the three 3-jet definition schemes proposed in section 3.2. The curves correspond to the exact 3-jet rates according to the 3-jet criteria in section 3.2.

In addition to these nominal 3-jet boundaries one also has to consider approximate "physical" 3-jet boundaries for the following reason. From the experience with e^+e^--interactions one knows that 3-jet events are starting to become discernable at $\sqrt{q^2}$=10 GeV. Correspondingly one does not expect to be able to discern 3-jet events in DIS much below W=10 GeV, and, if Q^2 sets the scale, much below $\sqrt{Q^2}$=10 GeV. We have indicated this in our plots by drawing dashed lines for $W \leq 10$ GeV and $Q \leq 10$ GeV. With our invariant mass cut of $y_{cut} = 0.04$ this would mean that we are cutting off at an invariant jet mass of ~ 2 GeV. These invariant mass cut-offs may have to be adjusted somewhat upward when one has gained more experinence with 3-jet detection in DIS at high energies. The corresponding changes in the invariant mass cuts can easily be effected in our figures.

Let us first comment on some common features of the curves Fig. 4-6. In the Figs. 4a, 5a, and 6a we display the dependence of the three-jet ratio R_3 on x for three values of Q^2. Apart from the x-dependence which is discussed later on one observes that one has $R_3(Q^2 = 10^4\text{GeV}^2) < R_3(Q^2 = 10^3\text{GeV}^2) < R_3(Q^2 = 10^2\text{GeV}^2)$ for all values of x. There are two sources of Q^2-dependencies in the 3-jet ratio R_3. Firstly one has the Q^2-dependence introduced through the evolving parton densities and secondly one has the Q^2-dependence from the running coupling constant $\alpha_s(Q^2)$. We have checked that the first source is negligible despite the fact that the Q^2-dependent parton densities enter differently in the numerator and denominator of R_3:

$$R_3(x,Q^2) \sim \frac{\alpha_s(Q^2)}{2\pi}\int\frac{dx_p}{x_p}\frac{\sum_p p(x/x_p,Q^2)\,D_p(x_p,x,Q^2)}{\sum'_{p'}p'(x,Q^2)\,C_{p'}(x,Q^2)} \tag{71}$$

Here D_p and C_p are (electro-weak dependent) terms containing the QCD content and we have approximated the denominator by the LL result. Yet, the Q^2-dependence tends to cancel among the numerator and denominator.

The pattern of increasing 3-jet fractions with decreasing Q^2 is mainly due to the fact that the 3-jet rate is proportional to the running coupling constant $\alpha_s(Q^2)$ which increases with decreasing Q^2. This is demonstrated also in Fig. 7 for the W-scheme where we plot the 3-jet fraction as a function of Q^2 keeping the strong coupling constant α_s at a fixed value of $\alpha_s(Q^2) = 300\text{GeV}^2$. The 3-jet fraction remains practically Q^2-independent over the whole Q^2-range which underpins our above assertion.

The pattern $R_3(W^2 = 10^4\text{GeV}^2) < R_3(W^2 = 10^3\text{GeV}^2) < R_3(W^2 = 10^2\text{GeV}^2)$ for any fixed value of x that is observed in Figs. 4b, 5b and 6b is also due mainly to the Q^2-dependence of the running coupling constant $\alpha_s(Q^2)$ since W^2 and Q^2 are proportional to each other for any fixed value of x viz. $Q^2 = xW^2/(1-x)$.

The same Q^2-dependence can also be seen in the curves of Figs. 4c, 5c and 6c where we plot the Q^2-dependence of the 3-jet rates for two values of x. Again the main source of Q^2-dependence is the strong coupling constant (see Fig. 7).

We now turn to the discussion of the x -dependencies of the 3-jet ratios shown in Figs. 4-6. These can be understood from the variation of the 3-jet phase space regions with x which is different for the three jet definition schemes proposed in section 3.2. We

recapitulate that the "mixed scheme" is defined by the requirement that the x_p and z integrations disentangle (see eq.(59)). In Fig. 6a and 6b we show the x-dependence of the 3-jet rate R_3 in this scheme. R_3 varies strongly with x for fixed Q^2 or fixed W^2. The steep increase of R_3 with decreasing x originates from the concurrent enlargement of the 3-jet region, compare Fig. 3c. Close to $x = 0$ the 3-jet cross section becomes large. R_3 may even exceed unity which would imply an (unrealistic) negative 2-jet rate for these x-values. One has to give up fixed order perturbation theory in this infrared sensitiv region and would have to invoke infrared exponentiation for the endpoint region.

In the Q-scheme the dependence of R_3 on x is even amplified. This results from the fact that the 3-jet region in the 3-parton phase space increases when x decreases (see Fig. 3b). Moreover its boundary also gets closer to the $z = 0$ and $z = 1$ poles which implies that more and more of the large $1/(z(1-z))$ terms contribute to the 3-jet cross section.

The opposite behaviour can be observed in the case of the "W-scheme", in which W^2 sets the scale for the jet definition. In this scheme the 3-jet rate R_3 is rather insensitive against variations in x. The x-distribution is essentially flat since the larger available phase space at small values of x is compensated by a larger contribution from the dominant $1/(1-x_p)$ term for large values of x. At both ends, $x = 0$ and $x = 1$, the x-distributions of R_3 vanishes since then the upper and lower x_p-integration limits become equal, see eq. (56).

In total we observe that the "W-scheme" seems to be most suitable for jet definition in leptoproduction. It provides a 3-jet rate which is nearly constant over a wide range of the overall kinematics (in x, Q^2 or W^2) and which, in particular, never exceeds unity so that the 2-jet rate always remains positive. From the point of view that fixed order perturbative QCD is only applicable as long as the correction terms are small, the W-scheme is the only one which satisfies this criterium for our choise of the y_{cut}-value. The $O(\alpha_s)$ effects can become large in the other schemes which indicates that higher order terms are necessary in order to obtain sensible results. The question, however, arises if the different x-behaviour of R_3 predicted by the different jet defining schemes "survives" the fragmentation and becomes experimentally observable. If so, an experimental analysis should be made to judge the relativ merits of the three jet definition schemes. This analysis is under study .

Note that one cannot use a jet definition scheme patterned after an experimental jet finding algorithm where one uses the condition that two hadrons should be combined if their invariant mass is below a *fixed* mass. This can be seen in Fig. 8 a and b where we show the 3-jet rate corresponding to the requirement $s_{ij} \geq 7\,\mathrm{GeV}^2$ as a function of x and Q^2. The boundaries of the 3 jet region for this jet definition scheme can be obtained from eq. (58) by the replacement $y_{cut} \to 7\mathrm{GeV}^2/Q^2$. This means, that the origins of the variation of R_3 with x for fixed Q^2 (Fig. 8a) and the variation of R_3 with Q^2 for fixed x (Fig. 8b) are the same as in the Q-scheme but the effects are strongly amplified for $Q^2 > 7\mathrm{GeV}^2/y_{cut}$. In addition the 3-jet phase space boundaries become Q^2-dependent which would be in competition with the Q^2 dependence of α_s that one would like to measure.

Let us finally mention that the fact that W sets the mass scale for the jet activity is in accordance with both the experimental [EMC] and theoretical [AM78, Mo81] observation that the mean transverse momentum of the quark produced in leptoproduction is given

by

$$< p_T^2 > \approx \text{const.}\, \alpha_s(Q^2) W^2$$

to a good approximation. Since a nonzero p_T (w.r.t. the current direction) becomes possible at the parton level only at $O(\alpha_s)$ the transverse momentum is obviously proportional to the separation of the two partons, i.e. provides a measure for the jet separation.

4 Summary

In this paper we have considered the complete $O(\alpha_s)$ corrections to leptoproduction as they are relevant for future *ep*-colliders like HERA. We have used dimensional regularization to regularize the IR/M and UV divergencies of massless QCD. Special care was taken to obtain the p.v. structure function F_3 in a consistent way. We have obtained the complete $O(\alpha_s)$ corrected electro-weak cross section formula both for the NC and the CC case. We defined parton densities according to the the standard scheme, where one require that the form of F_2 is unchanged to all orders of perturbation theory. Defining the K-factor as the ratio of the $O(\alpha_s)$ corrected cross section to the Born cross section we find that the K-factor deviates substantially from unity for very small values of x. This gives rise to some interesting physics which we have discussed in detail.

Jet definition in leptoproduction is less straightforward than in e^+e^- reactions. We discussed problems that arise in that context. We commented on the interplay of the jet characteristics and the initial state singularity, i.e. the effects coming from gluon emission *before* the hard collisions and the before-after interference effects. This leads to characteristic differences between the predictions of parton cascade models and full matrix element models which we have spelled out. Several theoretical jet definition schemes were proposed. Of these only the W-scheme leads to well behaved 3-jet and 2-jet rates. In the W-scheme the hadronic mass W^2 in the final hadronic CMS sets the mass scale for the jet invariant masses. In this scheme the 3-jet rate depends only very weakly on the kinematical variables x. Thus the $O(\alpha_s)$ corrections should allow for tests of perturbative aspects of QCD. Such an analysis would best be done with the help of a Monte Carlo generator where one can look for many jet-like measures like sphericity, thrust, energy flow, energy correlations, etc. . Furthermore we observe that the Q^2-dependence of the 3-jet rate is essentially governed by the strong coupling constant $\alpha_s(Q^2)$ for fixed x. In view of the large available Q^2-range at HERA the measurement of the Q^2-dependence of the 3-jet rate should thus provide a confirmation of the "running nature" of α_s over a large energy range. Clearly, to determine the mass scale of QCD, Λ_{QCD}, one needs the one-loop corrections. We are confident that the W-jet definition scheme will provide equally well behaved $O(\alpha_s^2)$ corrections to the 3-jet cross section. This in turn would allow for an independent determination of α_s in leptoproduction. Work on this subject is in progress.

Acknowledgements. We are grateful to Dr. G. Ingelman for helpful and interesting discussions.

A Appendix

In this Appendix we derive the relation between the hadronic and the partonic DIS structure functions eq. (23). The basic hypothesis is that the total cross section of a hadronic process can be written as the incoherent sum of the contributions of each parton type p within the hadron. Each of the parton carries a fraction η of the hadron total momentum (the gluon, $p = 0$, and n_f light quarks, $p = 1, \ldots, n_f$ and antiquarks, $p = -n_f, \ldots, -1$). In the case of DIS the hadronic cross section reads:

$$d\sigma_H(P) = \sum_{p=-n_f}^{n_f} \int_0^1 d\eta \, d\hat{\sigma}_p(\eta P) p_p^0(\eta) \tag{A.1}$$

Here $d\hat{\sigma}_p$ is the parton cross section corresponding to the parton p and $p_p^0(\eta)$ is the "bare" parton distribution function.

In the one-boson-exchange approximation it is convenient to specify the flavour dependent electro-weak coupling coefficients $A_f(Q^2)$ and $B_f(Q^2)$, (see eq. (12)). They multiply the parity conserving (pc) and parity violating (pv) part of the hadronic squared amplitude, respectively. Up to and including the $O(\alpha_s)$ contributions we can write:

$$d\sigma_H(P) = \sum_{f=1}^{n_f} \left\{ A_f(Q^2)\, d\sigma_{H,f}^{pc}(P) + B_f(Q^2)\, d\sigma_{H,f}^{pv}(P) \right\} \tag{A.2}$$

where ($p = \eta P$):

$$d\sigma_{H,f}^{pc/pv}(P) = \int_0^1 d\eta \, \left[q_f^0(\eta)\, d\hat{\sigma}_q^{pc/pv}(p) + \bar{q}_f^0(\eta)\, d\hat{\sigma}_{\bar{q}}^{pc/pv}(p) + G^0(\eta)\, d\hat{\sigma}_G^{pc/pv}(p) \right] \tag{A.3}$$

The partonic cross sections $d\hat{\sigma}_p$ are products of leptonic $L^{\mu\nu}$ and partonic tensors $W_{\mu\nu}$ (index $p = q, \bar{q}, G$):

$$\begin{aligned}
d\hat{\sigma}_p^A(p) &= \left[\frac{4\pi\alpha}{Q^2}\right]^2 \frac{1}{4p\cdot l} \frac{d^3l'}{2E'(2\pi)^3} 4\pi \, L_A^{\mu\nu} \, W_{\mu\nu}^{(p)A} \qquad (A = pc, pv) \qquad \text{(A.4)} \\
L_{pc}^{\mu\nu} &= 2\left(l^\mu l'^\nu + l'^\mu l^\nu - Q^2 \, g^{\mu\nu}/2\right) \\
L_{pv}^{\mu\nu} &= 2i\epsilon^{\mu\nu\alpha\beta} l_\alpha l'_\beta \\
W_{\mu\nu}(p,q)^{(p)pc/pv} &= \frac{1}{4\pi} \sum_N dPS^{(N)} H_{\mu\nu}^{(p)pc/pv}(p, q, p_1, \ldots, p_N)
\end{aligned}$$

Here $H_{\mu\nu}^{(p)}(N)$ is the spin-averaged square of the N-body final-state amplitude contributing to the virtual-boson-parton p process $q + p(p) \to p_1(f) + \ldots + p_N$. $PS^{(N)}$ is the corresponding N-body Lorentz-invariant phase space

$$PS^{(N)} = \int \prod_{i=1}^{N} \frac{d^{n-1}p_i}{(2\pi)^{n-1}} \frac{(2\pi)^n}{2E_i} \delta^n(p + q - \sum_{i=1}^{N} p_i)$$

Generalizing the lepton momentum integration in eq. (A.4) to n dimensions one has:

$$\frac{d^{n-1}l'}{2E'(2\pi)^{n-1}} = K(\epsilon) \frac{y^{s_p}}{16\pi^2} \, dy \, dx_p \tag{A.5}$$

where

$$\begin{aligned} s_p &= (p+l)^2 = \eta s \\ x_p &= \frac{Q^2}{2p\cdot q} \\ K(\epsilon) &= \left(\frac{Q^2(1-y}{4\pi}\right)^{-\epsilon} \frac{1}{\Gamma(1-\epsilon)} \end{aligned} \tag{A.6}$$

We can rewrite eq. (A.4) as follows ($A = pc, pv$):

$$d\hat{\sigma}_p^A = K(\epsilon)\frac{2\pi\alpha^2}{yQ^2}\, dy\, dx_p\, \frac{y}{x_p\eta s}\, L_A^{\mu\nu}\, W_{\mu\nu}^{(p)A} \tag{A.7}$$

Using the relation between the hadronic and partonic cross section eq. (A.1), considering that $\eta = x/x_p$, and taking into account the kinematical constraints we get ($A = pc, pv$):

$$\begin{aligned} d\sigma_{H,f}^A &= dy\, dx\, K(\epsilon)\frac{2\pi\alpha^2}{yQ^2}\int_x^1 \frac{dx_p}{x_p}\frac{y}{xs}\, L_A^{\mu\nu} \\ &\times \left\{ q_f^0(x/x_p)\, W_{\mu\nu}^{(q)A} + \bar{q}_f^0(x/x_p)\, W_{\mu\nu}^{(\bar{q})A} + G^0(x/x_p)\, W_{\mu\nu}^{(G)A} \right\} \end{aligned} \tag{A.8}$$

The parton tensor $W_{\mu\nu}^{(p)pc/pv}$ can be written in the usual structure function form:

$$\begin{aligned} W_{\mu\nu}^{(p)pc}(p,q) &= -\hat{g}_{\mu\nu}\frac{\mathcal{F}_1^{(p)}}{2} + \frac{\hat{p}_\mu\hat{p}_\nu}{p\cdot q}\, x_p\mathcal{F}_2^{(p)} \\ W_{\mu\nu}^{(p)pv}(p,q) &= \frac{-i}{p\cdot q}\,\epsilon_{\mu\nu\alpha\beta}q^\alpha p^\beta\,\frac{\mathcal{F}_3^{(p)}}{2} \end{aligned} \tag{A.9}$$

For the sake of convenience we have introduced the gauge completed hatted tensors

$$\begin{aligned} \hat{g}_{\mu\nu} &= g_{\mu\nu} + \frac{q_\mu q_\nu}{Q^2} \\ \hat{p}_\mu &= p_\mu + \frac{p\cdot q}{Q^2} q_\mu \end{aligned} \tag{A.10}$$

Contracting eq.(A.9) with the lepton tensor we find:

$$\begin{aligned} \frac{y}{xs} L_{pc}^{\mu\nu} W_{\mu\nu}^{(p,f)pc} &= \left[1 + (1-y)^2 - \epsilon y^2\right]\mathcal{F}_2^{(p)} - y^2\,\mathcal{F}_L^{(p)} \\ \frac{y}{xs} L_{pv}^{\mu\nu} W_{\mu\nu}^{(p,f)pv} &= y(2-y)\,\mathcal{F}_3^{(p)} \end{aligned} \tag{A.11}$$

where we have defined the n-dimensional longitudinal structure function F_L by:

$$\mathcal{F}_L^{(p)} \equiv (1-\epsilon)(\mathcal{F}_2^{(p)} - \mathcal{F}_1^{(p)}) \tag{A.12}$$

Note that the ϵ-dependent term proportional to $\mathcal{F}_2^{(p)}$ in eq. (A.11) has *not* been included in the definition of $\mathcal{F}_L^{(p)}$. This term, as well as the factor $(1-\epsilon)$ in eq. (A.12) arise from the n-dimensional contraction in eq. (A.11). Finally, inserting eq. (A.11) in eq. (A.8) and comparing with eq. (21) we find the relation between the hadronic and the partonic structure functions:

$$\mathcal{F}_{2,L,3}^f = \int_x^1 \frac{dx_p}{x_p}\left[q_f^0(x/x_p)\,\mathcal{F}_{2,L,3}^q + \bar{q}_f^0(x/x_p)\,\mathcal{F}_{2,L,3}^{\bar{q}} + G^0(x/x_p)\,\mathcal{F}_{2,L,3}^G \right] \tag{A.13}$$

Using the convolution $\otimes$, defined in eq. (24), we can rewrite the $O(\alpha_s)$ relation between the hadronic and partonic structure functions, eq. (A.13), as ($i = 2, L, 3$):

$$\mathcal{F}_i^f = q_f^0 \otimes \mathcal{F}_i^q + \bar{q}_f^0 \otimes \mathcal{F}_i^{\bar{q}} + G^0 \otimes \mathcal{F}_i^G \tag{A.14}$$

B Appendix

Here we derive the expressions needed to obtain the partonic structure functions $\mathcal{F}_{2,L,3}$ at next-to-leading order eqs. (28,29,30). We also present the fully differential cross section formula for the $O(\alpha_s)$ tree graph contributions. We assume the partons to be massless and work in $n = 4 - 2\epsilon$ dimensions.

(i) Naive parton model result for the partonic structure functions

We start with the Born process (4)

$$\text{virtual boson}(q) + \text{parton}(p) \rightarrow \text{parton}(p_1)$$

i.e. we are at $O(\alpha_s^0)$ and N equals $N = 1$ in eq. (A.4). In this simple case the phase space is given by:

$$dPS^{(1)} = \frac{2\pi x_p \delta(1-x_p)}{Q^2} \tag{B.1}$$

For the spin-averaged square of the amplitude one obtains:

$$\begin{aligned} H_{\mu\nu}^{(p)pc}(p,q) &= -\hat{g}_{\mu\nu}\, H_1^{(p)} + \frac{\hat{p}_\mu\hat{p}_\nu}{p\cdot q}\, H_2^{(p)} \\ H_{\mu\nu}^{(p)pv}(p,q) &= \frac{-i}{p\cdot q}\epsilon_{\mu\nu\alpha\beta}q^\alpha p^\beta\, H_3^{(p)} \end{aligned} \tag{B.2}$$

where the invariants $H_i^{(p)}$ read
quark initiated:

$$\begin{aligned} H_2^{(q)} &= H_3^{(q)} = 2Q^2 \\ H_L^{(q)} &\equiv (1-\epsilon)(H_2^{(q)} - 2x_p\, H_1^{(q)}) = 0 \end{aligned} \tag{B.3}$$

antiquark initiated:

$$\begin{aligned} H_{2,L}^{(\bar{q})} &= H_{2,L}^{(q)} \\ H_3^{(\bar{q})} &= -H_3^{(q)} \end{aligned} \tag{B.4}$$

With the definition of $W_{\mu\nu}$ eq. (A.4) the lowest order partonic structure functions are thus given by:
quark initiated:

$$\begin{aligned} \mathcal{F}_2^{(q)}[Born] &= \mathcal{F}_3^{(q)}[Born] = \delta(1-x_p) \\ \mathcal{F}_L^{(q)}[Born] &= 0 \end{aligned} \tag{B.5}$$

antiquark initiated:

$$\begin{aligned} \mathcal{F}_{2,L}^{(\bar{q})}[Born] &= \mathcal{F}_{2,L}^{(q)}[Born] \\ \mathcal{F}_{3}^{(\bar{q})}[Born] &= -\mathcal{F}_{3}^{(q)}[Born] \end{aligned} \tag{B.6}$$

(ii) Virtual $O(\alpha_s)$ QCD corrections to the partonic structure functions

To $O(\alpha_s)$ we have the real (tree graph) parton contributions (16) and the virtual (loop graph) corrections to the Born processes (4). The virtual corrections (1-parton final state, $N = 1$ in eq. (A.4)) factor the respective Born terms ($i = 2, L, 3$) [AEM79]:

$$\mathcal{F}_i^{(p)}[\text{virtual}] = \mathcal{F}_i^{(p)}[\text{Born}]\ \frac{\alpha_s C_F}{2\pi}\, C(\epsilon)\left(-\frac{2}{\epsilon^2} - \frac{3}{\epsilon} - 8 - \frac{\pi^2}{3}\right) \tag{B.7}$$

where

$$C(\epsilon) = \left(\frac{Q^2}{4\pi\mu^2}\right)^{-\epsilon} \frac{\Gamma(1-\epsilon)}{\Gamma(1-2\epsilon)} \tag{B.8}$$

Here $C_F = (N_C^2 - 1)/(2N_C)$ is the Casimir operator of the colour gauge group $SU(N_C)$.

(iii) Real $O(\alpha_s)$ QCD corrections to the partonic structure functions

For the real terms (2-parton final state, $N = 2$ in eq. (A.4)) besides x, Q^2 and x_p (which is trivial for the 1-parton case) we need two further kinematical variables to describe the cross sections. First we define Φ to be the azimuthal angle between the parton plane $(\vec{p}, \vec{p}_1)$ and the lepton plane $(\vec{l}, \vec{l}')$ in the cms $\vec{p} + \vec{q} = 0$. Second we introduce the scaling variable z defined by:

$$z = \frac{p \cdot p_1}{p \cdot q} \tag{B.9}$$

The 2-parton phase space can be written as:

$$dPS^{(2)} = \frac{C(\epsilon)}{1-2\epsilon}\,\frac{1}{8\pi}\, x_p^{\epsilon}(1-x_p)^{-\epsilon} z^{-\epsilon}(1-z)^{-\epsilon}\frac{dz}{N_z}\,\sin^{-2\epsilon}\Phi\,\frac{d\Phi}{N_\Phi} \tag{B.10}$$

where $N_\Phi = \pi 2^{2\epsilon}\Gamma(1-2\epsilon)/\Gamma^2(1-\epsilon)$ and $N_z = \Gamma^2(1-\epsilon)/\Gamma(2-2\epsilon)$ are normalization factors of the Φ and z integrations, respectively.

Next we expand the p.c. and p.v. spin-averaged square amplitudes for the real $O(\alpha_s)$ contributions

$$\text{virtual boson}(q) + \text{parton}(p) \rightarrow \text{parton}(p_1) + \text{parton}(p_2),$$

into a standard set of invariants:

$$\begin{aligned} H_{\mu\nu}^{(p)pc} &= -\hat{g}_{\mu\nu} H_1^{(p)} + \frac{1}{p\cdot q}\hat{p}_\mu\hat{p}_\nu H_2^{(p)} + \frac{1}{p\cdot q}\hat{p}_{1\mu}\hat{p}_{1\nu} H_3^{(p)} + \frac{1}{p\cdot q}(\hat{p}_\mu\hat{p}_{1\nu} + \hat{p}_{1\mu}\hat{p}_\nu) H_4^{(p)} \\ H_{\mu\nu}^{(p)pv} &= \frac{-i}{pq}\epsilon_{\mu\nu\alpha\beta} q^\alpha p^\beta H_6^{(p)} + \frac{i}{pq}\epsilon_{\mu\nu\alpha\beta} q^\alpha p_1^\beta H_7^{(p)} \end{aligned} \tag{B.11}$$

Note that the most general expansion includes one more p.c. structure function and two more p.v. structure functions. Since they obtain contributions only from imaginary parts of one-loop contributions [HHK82] they do not contribute at the $O(\alpha_s)$ level which we are considering in this paper.

Equivalently one can expand the hadronic tensor into 4 p.c. helicity invariants $H_\alpha^{(p)}$ ($\alpha = U+L, L, T, I$) and 2 p.v. helicity invariants $H_\alpha^{(p)}(\alpha = P, A)$. They are linearily related to the above set of invariants eq.(B.11). The relation between the two sets can be obtained by considering the contraction of the lepton tensors with the hadron tensor eq. (B.11). We evaluate the cross section in the c.m. frame of the virtual boson and the incoming parton, where (all partons are massless):

$$\begin{aligned} 2pp_1 = s_p y z \quad 2pp_2 = s_p y(1-z) \quad 2pq = s_p y \\ Q^2 = 2ll' = s_p y x_p \quad 2p_1p_2 = s_p y(1-x_p) \quad 2p_1 q = s_p y(1-x_p-z) \\ 2p_2 q = s_p y(z - x_p) \end{aligned}$$

The azimuthal angle Φ is specified by

$$2lp_1/s_p = (1-y)z x_p + (1-z)(1-x_p) + 2\cos\Phi\sqrt{(1-y)z(1-z)x_p(1-x_p)}.$$

One finds:

$$\begin{aligned} \frac{y}{s_p} L_{pc}^{\mu\nu} H_{\mu\nu}^{(p)pc} &= \left[1 + (1-y)^2 - \epsilon y^2\right] H_{U+L}^{(p)} - y^2 H_L^{(p)} \\ &\quad + 2(1-y)\cos 2\Phi\ H_T^{(p)} + (2-y)\sqrt{1-y}\,cos\Phi\ H_I^{(p)} \\ \frac{y}{s_p} L_{pv}^{\mu\nu} H_{\mu\nu}^{(p)pv} &= y(2-y) H_P^{(p)} - 4y\sqrt{1-y}\,\cos\Phi\ H_A^{(p)} \end{aligned} \tag{B.12}$$

Here we have introduced the following six linear combinations $H_\alpha^{(p)}$ of the structure functions $H_i^{(p)}$ ($\alpha \in \{U+L, L, T, I, P, A\}$):

$$\begin{aligned} H_{U+L}^{(p)} &= H_2^{(p)} + \left(2h_2 + h_1^2\right) H_3^{(p)} + 2h_1 H_4^{(p)} \\ H_L^{(p)} &= (1-\epsilon)(-2x_p H_1^{(p)} + H_2^{(p)} + h_1^2 H_3^{(p)} + 2h_1 H_4^{(p)}) - \epsilon\, 2h_2 H_3^{(p)} \\ H_T^{(p)} &= 2h_2 H_3^{(p)} \\ H_I^{(p)} &= 4\sqrt{h_2}\,(h_1 H_3^{(p)} + H_4^{(p)}) \\ H_P^{(p)} &= 2x_p(H_6^{(p)} - h_1 H_7^{(p)}) \\ H_A^{(p)} &= 2x_p\sqrt{h_2}\, H_7^{(p)} \end{aligned} \tag{B.13}$$

Explicit $O(\alpha_s)$ expressions for the H_i are given in App. C. We have also used the abbreviations :

$$\begin{aligned} h_1 &= (1-x_p)(1-z) + x_p z \\ h_2 &= x_p(1-x_p)z(1-z) \end{aligned} \tag{B.14}$$

The quantities $H_\alpha^{(p)}$ are related to helicity cross sections:

$$4x_p g^2 \frac{d^2\sigma_p^\alpha}{dx_p dz} = H_\alpha^{(p)} \tag{B.15}$$

The helicity cross sections $d\sigma_p^\alpha$ are the n-dimensional counter parts of the 4-dimensional helicity cross sections as defined e.g. in [KR81]. Explicite expressions for the helicity cross sections are given in App. C. With their help we finally arrive at the tree graph hadronic cross section to $O(\alpha_s)$[11]:

$$\begin{aligned} d\sigma_H &= \frac{K(\epsilon)C(\epsilon)}{1-2\epsilon}\frac{2\pi\alpha^2}{yQ^2}\frac{\alpha_s}{2\pi}dydx\int_x^1\frac{dx_p}{x_p}x_p^\epsilon(1-x_p)^{-\epsilon}\int_0^1\frac{dz}{N_z}z^{-\epsilon}(1-z)^{-\epsilon} \\ &\quad\times\int_0^\pi \sin^{-2\epsilon}\Phi\frac{d\Phi}{N_\Phi}\{I_G+I_q\} \end{aligned} \tag{B.16}$$

where

$$\begin{aligned} I_G &= p_G^0(x/x_p)\left\{\left(\sum_{f=1}^{N_f}A_f(Q^2)\right)\sum_{\alpha=U+L,L,T,I}g_\alpha(y,\Phi)\frac{d^2\sigma_G^\alpha}{dx_pdz}\right. \\ &\quad\left.+\left(\sum_{f=1}^{N_f}B_f(Q^2)\right)\sum_{\alpha=P,A}g_\alpha(y,\Phi)\frac{d^2\sigma_G^\alpha}{dx_pdz}\right\} \end{aligned} \tag{B.17}$$

and

$$\begin{aligned} I_q &= \sum_{f=1}^{\min(N_f,n_f)}\left\{\left[q_f^0(x/x_p)+\bar{q}_f^0(x/x_p)\right]A_f(Q^2)\left(\sum_{\alpha=U+L,L,T,I}g_\alpha(y,\Phi)\frac{d^2\sigma_q^\alpha}{dx_pdz}\right)\right. \\ &\quad\left.+\left[q_f^0(x/x_p)-\bar{q}_f^0(x/x_p)\right]B_f(Q^2)\left(\sum_{\alpha=P,A}g_\alpha(y,\Phi)\frac{d^2\sigma_q^\alpha}{dx_pdz}\right)\right\} \end{aligned} \tag{B.18}$$

The y and Φ dependent factors $g_\alpha(y,\Phi)$ are defined by:

$$\begin{aligned} g_{U+L}(y,\Phi) &= 1+(1-y)^2-\epsilon y^2 \\ g_L(y,\Phi) &= -y^2 \\ g_T(y,\Phi) &= 2(1-y)\cos 2\Phi \\ g_I(y,\Phi) &= \sqrt{1-y}(2-y)\cos\Phi \\ g_P(y,\Phi) &= y(2-y) \\ g_A(y,\Phi) &= -4y\sqrt{1-y} \end{aligned} \tag{B.19}$$

We have also made use of the fact that the antiquark helicity cross sections are equal (opposite equal) to the quark helicity cross sections in the p.c. (p.v.) case.

After Φ integration H_T, H_I and H_A do not contribute to the DIS cross section and H_{U+L}, H_L and H_P will result in the usual structure functions $\mathcal{F}_2$, $\mathcal{F}_L$ and $\mathcal{F}_3$ respectively.

$$\mathcal{F}_{2,L,3}^{(p)}[\text{real}] = C(\epsilon)\frac{\alpha_s}{2\pi}x_p^\epsilon(1-x_p)^{-\epsilon}\int_0^1 d\tilde{z}\,\frac{d^2\sigma_p^{U+L,L,P}}{dx_pdz} \tag{B.20}$$

Here the measure $d\tilde{z}$ is defined by:

$$d\tilde{z} = z^{-\epsilon}(1-z)^{-\epsilon}\frac{dz}{(1-2\epsilon)N_z} \tag{B.21}$$

[11]The 4-dimensional expressions agree with those in e.g. [Me78, PR80, FP82].

The z-integration yields IR/M divergent expressions. The singularities show up as poles in $1/\epsilon$. Since the x_p-integration yields further $1/\epsilon$-poles, we need to do the z-integrations up to order ϵ. Performing the z-integrations we obtain (q- and $\bar{q}$- cross sections are equal for $\sigma^{U+L,L}$, opposite equal for σ^P):

$$\begin{aligned} \int_0^1 d\tilde{z}\frac{d^2\sigma_q^{U+L}}{dx_pdz} &= \frac{C_F}{1-x_p}\left(\frac{-1}{\epsilon}(1+x_p^2)+\frac{3}{2}-x_p-2x_p^2-\frac{7}{2}\epsilon\right) \\ \int_0^1 d\tilde{z}\frac{d^2\sigma_q^{L}}{dx_pdz} &= C_F\,2x_p \\ \int_0^1 d\tilde{z}\frac{d^2\sigma_q^{P}}{dx_pdz} &= -C_F(1+x_p)+\int_0^1 d\tilde{z}\frac{d^2\sigma_q^{U+L}}{dx_pdz} \end{aligned} \tag{B.22}$$

and

$$\begin{aligned} \int_0^1 d\tilde{z}\frac{d^2\sigma_H^{U+L}}{dx_pdz} &= 2T_R\left(\frac{1-2x_p(1-x_p)}{-\epsilon}+6x_p(1-x_p)\right) \\ \int_0^1 d\tilde{z}\frac{d^2\sigma_H^{L}}{dx_pdz} &= 2T_R\,4x_p(1-x_p) \\ \int_0^1 d\tilde{z}\frac{d^2\sigma_H^{P}}{dx_pdz} &= 0 \end{aligned} \tag{B.23}$$

The x_p-integrations, on the other hand, cannot be done analytically since the parton densities are also x_p-dependent (see eq. (24)). However, we want to make the IR/M singularities in the tree graph contributions manifest. To this end we use the modified "+ distribution", the so called "$A+$ distribution" defined by:

$$\begin{aligned} \int_A^1\frac{h(x_p)dx_p}{(1-x_p)_{A+}} &\equiv \int_A^1\frac{h(x_p)-h(1)}{1-x_p}dx_p \\ \int_A^1 h(x_p)\left(\frac{\ln(1-x_p)}{1-x_p}\right)_{A+} &\equiv \int_A^1[h(x_p-h(1)]\frac{\ln(1-x_p)}{1-x_p}dx_p \end{aligned} \tag{B.24}$$

This $A+$ distribution is necessary since we encounter integrals in the range $[x,1]$. For $A=0$ the $A+$ distribution coincides with the usual + distribution [AEM79]. With the help of the $A+$ distribution we obtain the following expansion:[12]

$$\begin{aligned} x_p^\epsilon(1-x_p)^{-1-\epsilon} &= \delta(1-x_p)\left\{\frac{-1}{\epsilon}+\ln(1-A)-\frac{\epsilon\ln^2(1-A)}{2}\right\} \\ &\quad+\frac{1}{(1-x_p)_{A+}}-\epsilon\left(\frac{\ln(1-x_p)}{1-x_p}\right)_{A+}+\frac{\epsilon\ln x_p}{1-x_p} \end{aligned} \tag{B.25}$$

For the quark initiated cross sections a straightforward calculation yields:

$$\begin{aligned} \mathcal{F}_2^{(q)}[\text{real}] &= \frac{\alpha_s}{2\pi}\left\{C_FC(\epsilon)\,\delta(1-x_p)\left(\frac{2}{\epsilon^2}+\frac{3}{\epsilon}+8+\frac{\pi^2}{3}\right)+\frac{C(\epsilon)}{\epsilon}P_{qq}(x,x_p)+f_2^q(x,x_p)\right\} \\ \mathcal{F}_L^{(q)}[\text{real}] &= \frac{\alpha_s}{2\pi}C_F\,2x_p \\ \mathcal{F}_3^{(q)}[\text{real}] &= -\frac{\alpha_s}{2\pi}C_F(1+x_p)+\mathcal{F}_2^{(q)}[\text{real}] \end{aligned} \tag{B.26}$$

[12]Note that the right side of this expansion depends on the lower bound of the x_p-integartion

Here we have defined:

$$P_{qq}(x,x_p) = C_F\left\{\frac{1+x_p^2}{(1-x_p)_{z+}}+\delta(1-x_p)\left[\frac{3}{2}+2\ln(1-x)\right]\right\} \quad (B.27)$$

$$f_2^q(x,x_p) = C_F\left\{(1+x_p^2)\left[\left(\frac{\ln(1-x_p)}{1-x_p}\right)_{z+}-\frac{\ln x_p}{1-x_p}\right]+2x_p+3-\frac{3}{2}\frac{1}{(1-x_p)_{z+}}\right.$$
$$\left.+\delta(1-x_p)\left[\ln^2(1-x)-\frac{3}{2}\ln(1-x)-\frac{9}{2}-\frac{\pi^2}{3}\right]\right\}$$

Again, the antiquark structure functions are equal (opposite equal) to the quark structure functions for $i=2,L$ ($i=3$). $C(\epsilon)$ is defined in eq.(B.8).
For the gluon initiated parton cross section we find:

$$\frac{1}{2}\mathcal{F}_2^{(G)}[\text{real}](x_p,Q^2) = \frac{\alpha_s}{2\pi}\left[\frac{-C(\epsilon)}{\epsilon}P_{qG}(x_p)+f_2^G(x_p)\right] \quad (B.28)$$

$$\frac{1}{2}\mathcal{F}_L^{(G)}[\text{real}](x_p) = \frac{\alpha_s}{2\pi}T_R\,4x_p(1-x_p)$$

$$\frac{1}{2}\mathcal{F}_3^{(G)}[\text{real}](x_p,Q^2) = 0$$

where

$$P_{qG}(x_p) = T_R\left[x_p^2+(1-x_p)^2\right] \quad (B.29)$$

$$f_2^G(x_p) = T_R\left\{\left[x_p^2+(1-x_p)^2\right]\ln\frac{1-x_p}{x_p}+6x_p(1-x_p)\right\}$$

(iv) Total $O(\alpha_s)$ correction to the partonic structure functions

We now add up the respective Born, virtual and real $O(\alpha_s)$ terms to obtain the total $O(\alpha_s)$ corrected (partonic) structure functions $\mathcal{F}_i^{(p)}$ ($i=2,L,3$). Since the Born term and virtual contributions to the gluon initiated process are zero, the total corrections to the gluonic structure functions are identical to the pure real terms eq. (B.28):

$$\mathcal{F}_i^{(G)}[\alpha_s](x_p,Q^2) \equiv \mathcal{F}_i^{(G)}[\text{Born}+\text{real}+\text{virtual}](x_p,Q^2) \quad (B.30)$$
$$= \mathcal{F}_i^{(G)}[\text{real}](x_p,Q^2)$$

The corresponding sum of the quark (antiquark) inititated process is [13]:

$$\mathcal{F}_2^{(q)}[\alpha_s](x,x_p,Q^2) = \mathcal{F}_2^{(q)}[\alpha_s](x,x_p,Q^2) \quad (B.31)$$
$$= \delta(1-x_p)+\frac{\alpha_s}{2\pi}\left[\frac{-C(\epsilon)}{\epsilon}P_{qq}(x_p)+f_2^q(x,x_p)\right]$$

$$\mathcal{F}_L^{(q)}[\alpha_s](x_p) = \mathcal{F}_L^{(q)}[\alpha_s](x_p)$$
$$= \frac{\alpha_s C_F}{2\pi}2x_p$$

$$\mathcal{F}_3^{(q)}[\alpha_s](x,x_p,Q^2) = -\mathcal{F}_3^{(q)}[\alpha_s](x,x_p,Q^2)$$
$$= \mathcal{F}_2^{(q)}[\alpha_s](x,x_p,Q^2)-\frac{\alpha_s C_F}{2\pi}(1+x_p)$$

[13] Here we can explicitly see the remaining mass singularity.

Note that the Q^2-dependence originates from the expansion of $C(\epsilon)$ via:

$$\frac{-C(\epsilon)}{\epsilon} = \ln\frac{Q^2}{\mu^2}-\frac{1}{\epsilon}+\gamma-\ln 4\pi$$

where μ is an arbitrary mass scale introduced to keep the coupling dimesionless and γ is the Euler constant.

C Appendix

Here we shall write down the $O(\alpha_s)$ expressions of the tree graph hadron tensors. We have found it most convenient to derive these from crossing the relevant $e^+e^- - q\bar{q}g$ expressions given e.g. in [KS87]. Since we want to eventually integrate the partonic cross sections over their respective IR/M regions and control the IR/M divergencies by dimensional regularization, the tensors have to be calculated to $O(\epsilon)$ accuracy when necessary.

We shall first discuss the p.c. case. The quark-initiated hadron tensors are obtained from the e^+e^--case by the replacement $p_1\to p_1$, $p_2\to -p$, $p_3\to p_2$, $H_{\mu\nu}\to -H_{\mu\nu}$ and $g^2C_FN_C\to\frac{1}{2}g^2C_F$ where now p[initial quark] $=p$, p[final quark] $=p_1$, $p_G=p_3$. One has

$$H_1^{(q)} = g^2C_F\frac{2}{(1-x_p)(1-z)}\left(1+(1-z-x_p)^2-\epsilon(z-x_p)^2\right) \quad (C.1)$$

$$H_2^{(q)} = H_3^{(q)} = g^2C_F(1-\epsilon)\frac{4x_p}{(1-x_p)(1-z)}$$

$$H_4^{(q)} = g^2C_F\,\epsilon\frac{4x_p}{(1-x_p)(1-z)}$$

This leads to the cross section expressions

$$\frac{d^2\sigma_q^{U+L}}{dx_p dz} = C_F\left[\frac{1+x_p^2z^2}{(1-x_p)(1-z)}+(1-x_p)(1-z)+4x_pz\right. \quad (C.2)$$
$$\left.-\epsilon\left(\frac{1-x_p}{1-z}+\frac{1-z}{1-x_p}\right)\right]$$

$$\frac{d^2\sigma_q^L}{dx_p dz} = C_F 4x_pz$$

$$\frac{d^2\sigma_{q,i}^T}{dx_p dz} = C_F 2x_pz$$

$$\frac{d^2\sigma_{q,i}^T}{dx_p dz} = C_F\frac{-4h_1\sqrt{h_2}}{(1-x_p)(1-z)}$$

We have left out $O(\epsilon)$ terms that do not ultimately lead to finite contributions. The antiquark-initiated process is described by identical expressions where now of course the outgoing antiquark labels the final parton momentum p_1.

The gluon initiated hadron tensor can be obtained from the e^+e^--case by the replacement $p_1\to p_1$, $p_2\to p_2$, $p_3\to -p$, $H_{\mu\nu}\to H_{\mu\nu}$ and $g^2C_FN_C\to\frac{1}{2}g^2T_R$. The invariants H_i read ($T_R=\frac{1}{2}$)

$$H_1^{(G)} = 2g^2T_R\frac{1}{z(1-z)}\left((1-z-x_p)^2+(z-x_p)^2-\epsilon\right) \quad (C.3)$$

$$H_2^{(G)} = 2g^2T_R(1-\epsilon)\frac{2x_p}{z(1-z)}$$
$$H_3^{(G)} = 4g^2T_R\frac{2x_p}{z(1-z)}$$
$$H_4^{(G)} = -2g^2T_R\frac{2x_p}{z(1-z)}$$

For the cross sections one has

$$\frac{d^2\sigma_G^{U+L}}{dx_p dy} = T_R\left[\left(\frac{1}{z}+\frac{1}{1-z}-2\right)[1-\epsilon-2x_p(1-x_p)]+8x_p(1-x_p)-2\epsilon\right] \quad \text{(C.4)}$$
$$\frac{d^2\sigma_G^{L}}{dx_p dy} = T_R\left[8x_p(1-x_p)\left(1-\frac{3}{2}\epsilon\right)\right]$$
$$\frac{d^2\sigma_G^{T}}{dx_p dy} = T_R\left[4x_p(1-x_p)\right]$$
$$\frac{d^2\sigma_G^{I}}{dx_p dy} = T_R\left[\frac{-4(2x_p-1)(2z-1)\sqrt{h_2}}{z(1-z)}\right]$$

The calculation of the parity-violating hadronic tensor requires some care due to the presence of γ_5 in the context of an n-dimensional regularization of IR/M singularities [KKLS85]. As in [KKLS86] we shall use the BM γ_5-regularization scheme [BM77], which, to our knowledge, provides the only consistent γ_5-dimensional regularization scheme.

Because chiral invariance no longer holds true at the $O(\epsilon)$ level even for mass zero-quarks the p.v. cross section has to be defined symetrically by $H_{\mu\nu}^{pv} = \frac{1}{2}(V_\mu A_\nu^* + A_\mu V_\nu^*)$, where V_μ and A_μ denote the relevant vector and axial vector current matrix elements.

The quark initiated process can again be obtained again by crossing from the corresponding e^+e^--case [KKLS86]:

$$H_{q\,\mu\nu}^{pv} = 2g^2C_F\frac{1}{pq}\frac{1}{(1-x_p)(1-z)}\left[(1-\epsilon(1-z))\,i\epsilon_{\mu\nu\alpha\beta}q^\alpha p^\beta - \right. \quad \text{(C.5)}$$
$$\left.((1-x_p-z)-\epsilon(1-x_p))\,i\epsilon_{\mu\nu\alpha\beta}q^\alpha p_1^\beta + \epsilon(z-x_p)i\epsilon_{\mu\nu\alpha\beta}p^\alpha p_1^\beta\right] + \epsilon\hat{R}_{\mu\nu}$$

As is apparent from the third term in the square-brackets the p.v. Born term contribution eq. (C.5) is not conserved at the $O(\epsilon)$ level, i.e. $q^\mu H_{\mu\nu}^{pv}$ (Born) $\neq 0$. Note that this nonconserved piece will finally yield a finite contribution after IR/M integration. Its contribution to the helicity cross section G_p may be obtained by noting that

$$i\epsilon^{\mu\nu\alpha\beta}l_\alpha l'_\beta i\epsilon_{\mu\nu\alpha\beta}p^\alpha p_1^\beta = \frac{1}{2}is_p^2x_pzy(y-2) \quad \text{(C.6)}$$

whereas its contribution to G_A remains of $O(\epsilon)$ even after IR/M integration.

One may worry that a different choice of electro-weak gauge (differing from the Feynman gauge used here) could lead to an ultimately finite gauge dependent contribution of the nonconserved piece. However, as shown in [KKLS85] nonvanishing, gauge dependent contributions, as e.g. in $q^\nu H_{\mu\nu}^{pv} \neq 0$, vanish after IR/M integration.

We have not explicitly written out the remaining piece $\epsilon\hat{R}_{\mu\nu}$ which is given in [KKLS86] for the corresponding e^+e^--case. Since its cross section contribution is determined by a

contraction with the lepton tensor $\epsilon^{\mu\nu\alpha\beta}l_\alpha l'_\beta$, one finds that only the 4-dimensional part of $\hat{R}_{\mu\nu}$ contributes to the cross section as specified in the BM scheme. However, in 4 dimensions $\hat{R}_{\mu\nu} \equiv 0$ due to the validity of Schouten's identity [KKLS85]. Concerning a possible gauge dependent contribution of $R_{\mu\nu}$ the same remarks as above apply. In the following we shall therefore no longer list the $\hat{R}_{\mu\nu}$-contribution.

The antiquark initiated hadron tensor can be obtained from eq. (C.5) by antisymmetrization, i.e.

$$H_{\bar{q}\mu\nu}^{pv}(p,p_1) = -H_{q\mu\nu}^{pv}(p_1,p) \quad \text{(C.7)}$$

For the gluon initiated Born term contribution one has

$$H_{G\mu\nu}^{pv} = -2g^2T_R\frac{1}{pq}\left[\left(\frac{1-z-x_p}{z(1-z)}+\frac{\epsilon}{1-z}\right)i\epsilon_{\mu\nu\alpha\beta}q^\alpha p_1^\beta - \right. \quad \text{(C.8)}$$
$$\left.\left(\frac{z-x_p}{z(1-z)}+\frac{\epsilon}{z}\right)i\epsilon_{\mu\nu\alpha\beta}q^\alpha p_2^\beta + \epsilon\frac{1}{z(1-z)}i\epsilon_{\mu\nu\alpha\beta}p_1^\alpha p_2^\beta\right]$$

We have not written the gluon initiated hadron tensor in the standard form eq. (B.11) in order to make the quark-antiquark ($z \leftrightarrow (1-z)$) antisymmetry manifest. The $q-\bar{q}$ antisymmetry implies that flavour tagging is required if one wants to detect the gluon initiated cross section part. In the same vein, the IR/M integration of the gluon initiated cross section gives a zero result since one is not differentiating between quark and antiquark in the IR/M integration.

For the p.v. cross section we finally obtain

quark initiated:

$$\frac{d^2\sigma_q^P}{dx_p dz} = -C_F\left[2(1-x_p)(1-z)+4x_pz\right]+\frac{d^2\sigma_q^{U+L}}{dx_p dz} \quad \text{(C.9)}$$
$$\frac{d^2\sigma_q^A}{dx_p dz} = C_F\sqrt{h_2}\left(\frac{1-z-x_p}{(1-x_p)(1-z)}\right)$$

antiquark initiated:

$$\frac{d^2\sigma_{\bar{q}}^{P,A}}{dx_p dz} = -\frac{d^2\sigma_q^{P,A}}{dx_p dz} \quad \text{(C.10)}$$

gluon initiated:

$$\frac{d^2\sigma_G^P}{dx_p dz} = T_R(1-2x_p(1-x_p)+\epsilon)\frac{z-(1-z)}{z(1-z)} \quad \text{(C.11)}$$
$$\frac{d^2\sigma_G^A}{dx_p dz} = T_R\sqrt{h_2}\left(\frac{1-z-x_p}{z(1-z)}+\frac{z-x_p}{z(1-z)}+2\frac{\epsilon}{1-z}\right)$$

At first sight it is surprising that $d\sigma_G^A$ exhibits no manifest $q \leftrightarrow \bar{q}$ ($z \leftrightarrow (1-z)$)antisymmetry. This may be traced to the definition of the azimuthal angle Φ which is measured from the quark's momentum.

Figure 1: a) Zeroth order diagrams for lepton-parton scattering.
b)-d) Real (tree graph) $O(\alpha_s)$ corrections: b) quark initiated, c) boson-gluon fusion, d) antiquark initiated.
e) Kinematic diagram for three-jet production.

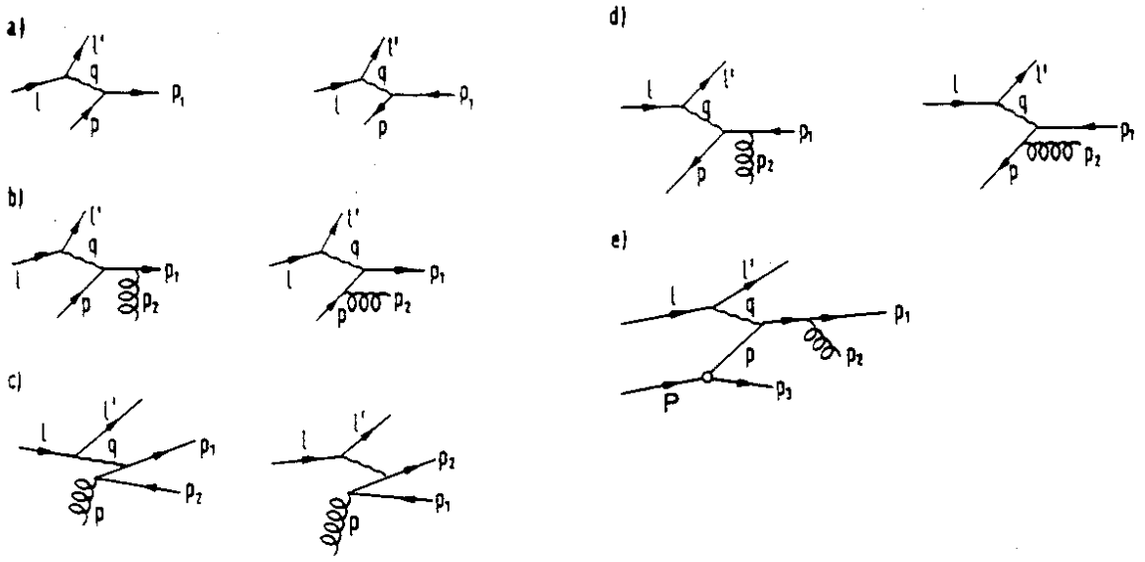

Figure 2: $O(\alpha_s)$ K-factor for NC and CC e^-p-scattering at HERA cms energy ($\sqrt{s}$=314GeV) as a function of Q^2 for different values of x.

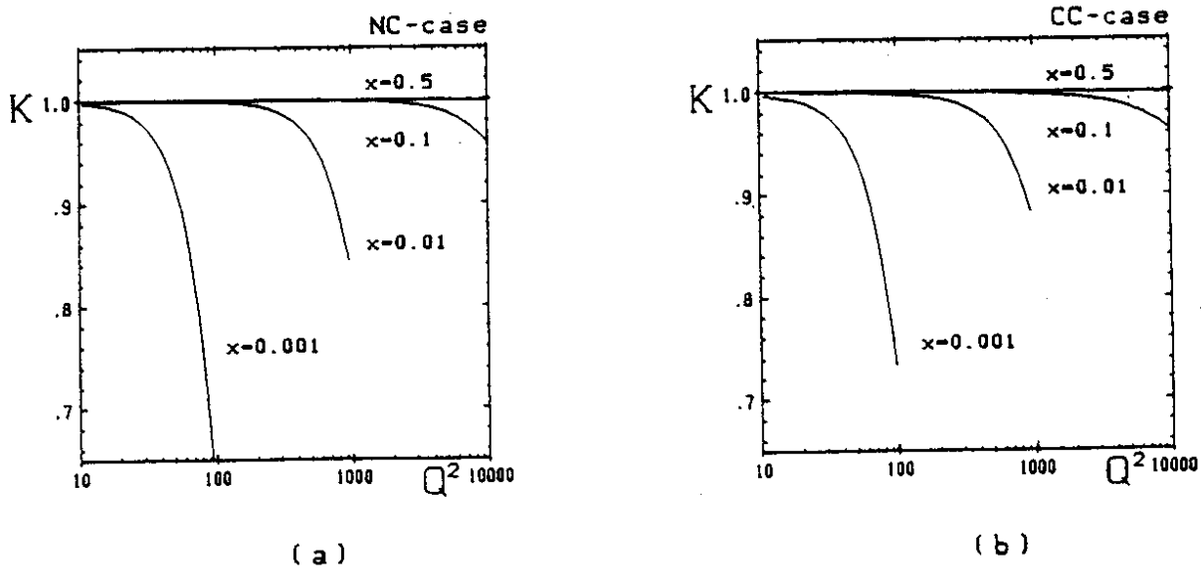

Figure 3: Genuine 3-jet region (shaded area) of the 3-parton phase space for various jet definition schemes and for two values of x (x=0.1 and x=0.5).
a) W-scheme b) Q-scheme c) mixed-scheme

a)

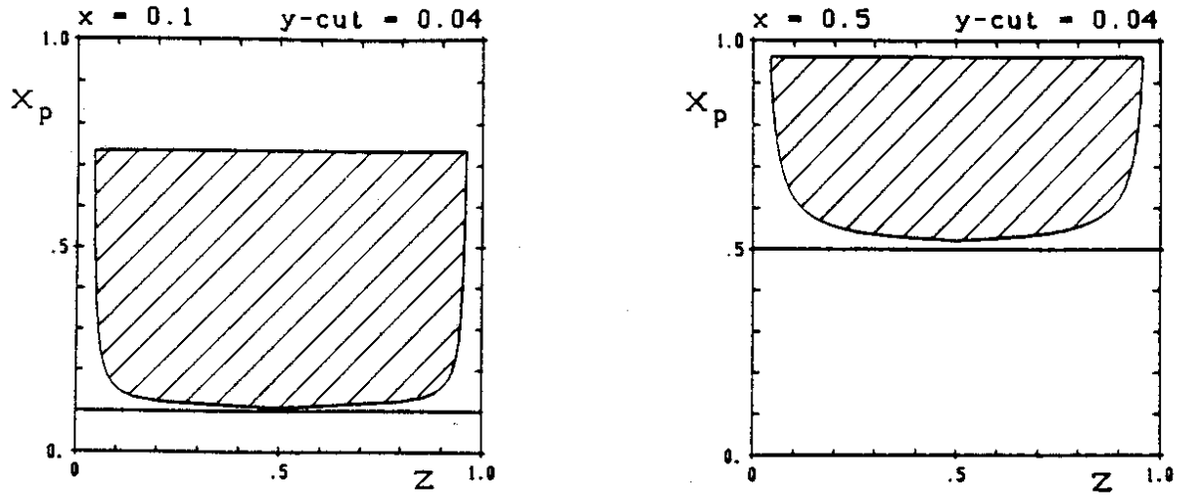

b)

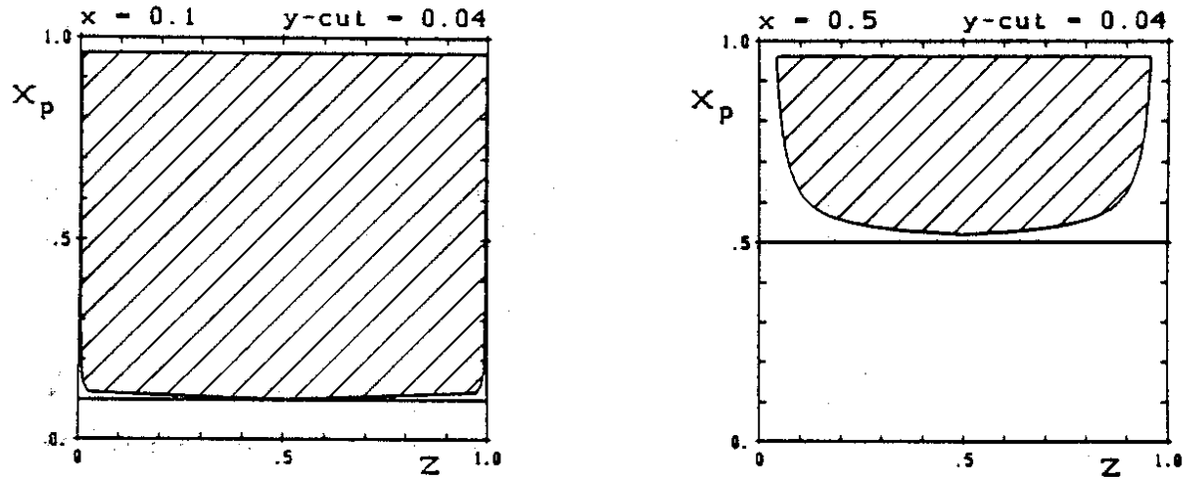

c)

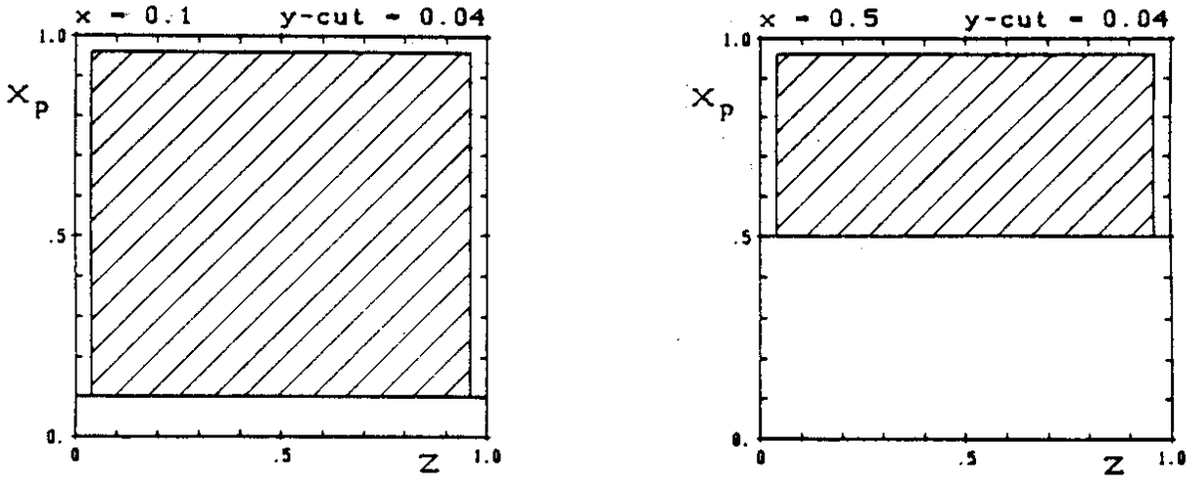

Figure 4: The ratio R_3 of 3-jet events over the total $O(\alpha_s)$ cross section for the W-scheme as a function of x for various Q^2 and W^2 values and as a function of Q^2 for various x values. (— : $W^2 \geq 100\,\mathrm{GeV}^2$ - - - : $W^2 < 100\,\mathrm{GeV}^2$)

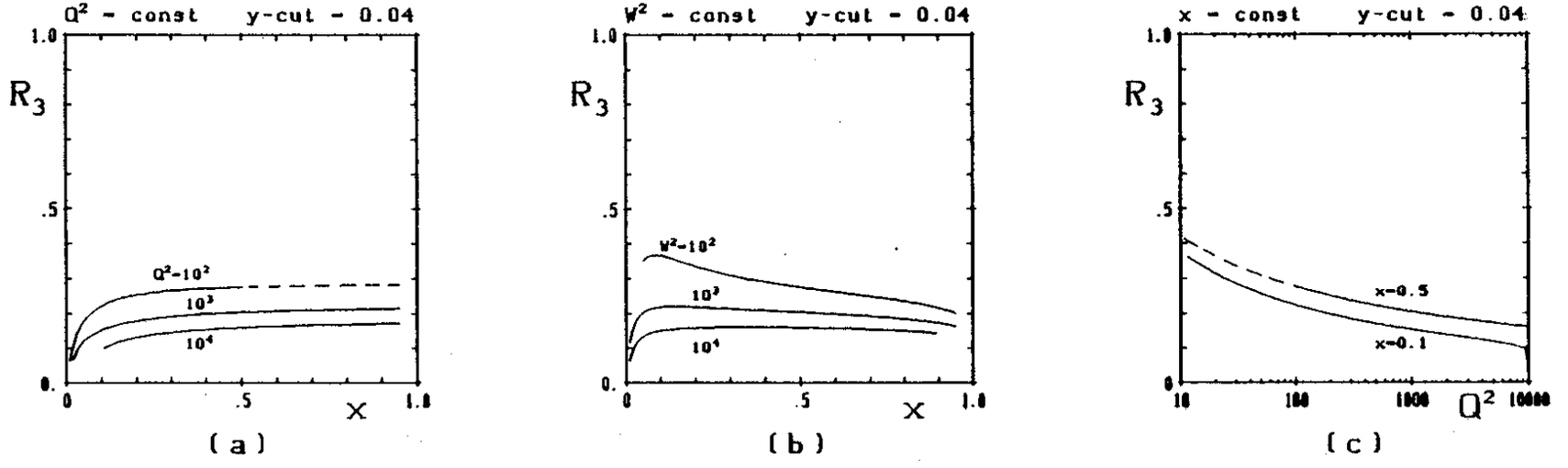

Figure 5: The ratio R_3 of 3-jet events over the total $O(\alpha_s)$ cross section for the Q-scheme as a function of x for various Q^2 and W^2 values and as a function of Q^2 for various x values. (— : $Q^2 \geq 100\,\mathrm{GeV}^2$ - - - : $Q^2 < 100\,\mathrm{GeV}^2$)

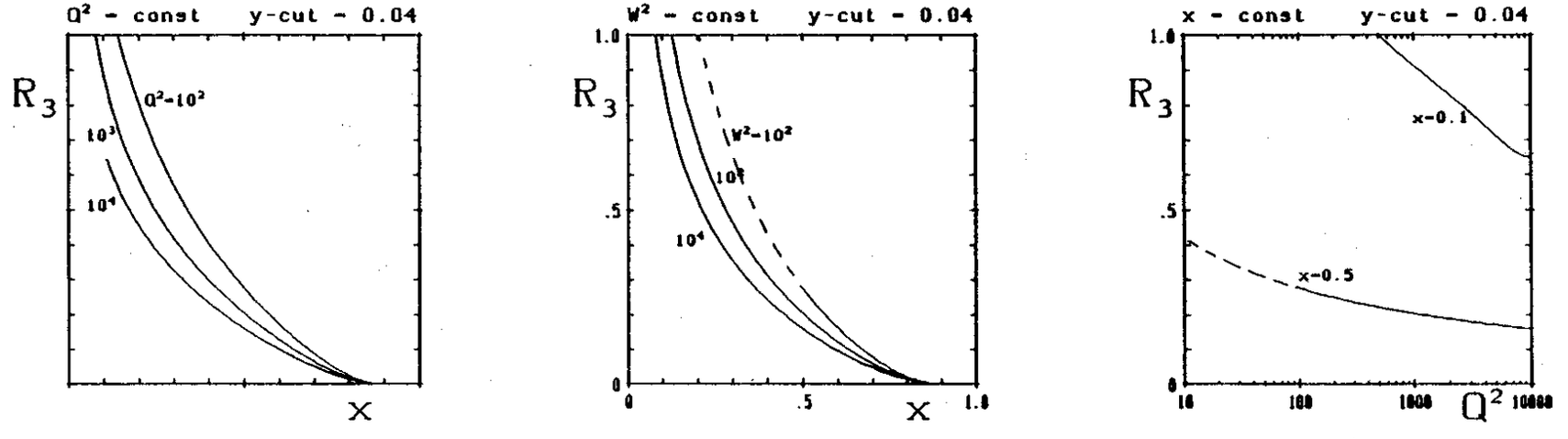

Figure 6: The ratio R_3 of 3-jet events over the total $O(\alpha_s)$ cross section for the mixed-scheme as a function of x for various Q^2 and W^2 values and as a fucntion of Q^2 for various x values. (— : $Q^2 \geq 100\,\mathrm{GeV}^2$ - - - : $Q^2 < 100\,\mathrm{GeV}^2$)

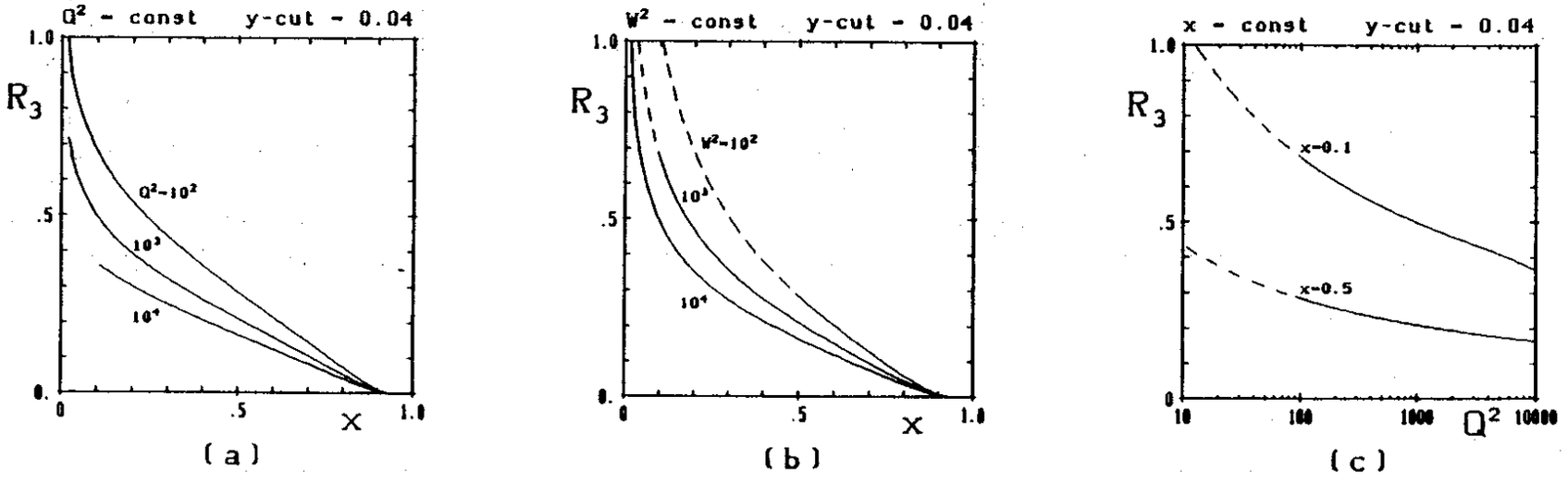

Figure 7: The ratio R_3 of 3-jet events over the total $O(\alpha_s)$ cross section for the W - scheme as a function of Q^2 for a given fixed coupling constant $\alpha_s(Q^2 = 300\text{GeV}^2)$ and for a running coupling constant $\alpha_s(Q^2)$.

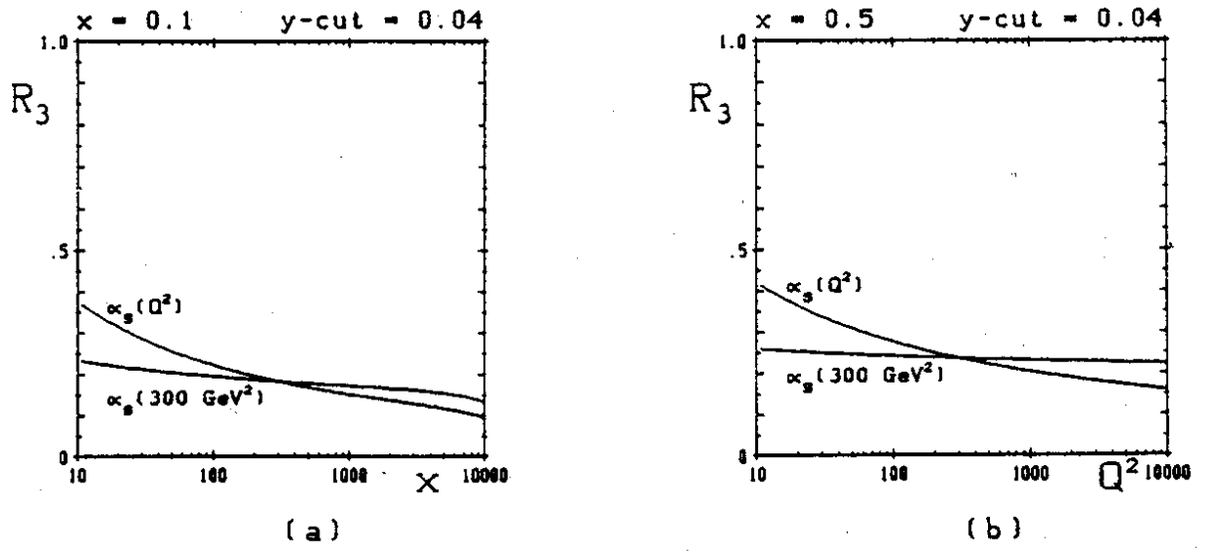

Figure 8: The ratio R_3 of 3-jet events over the total $O(\alpha_s)$ cross section for a jet definition scheme corresponding to the requirement $s_{ij} \geq 7\text{GeV}^2$ as a function of x for various Q^2 values and as a function of Q^2 for various x values.

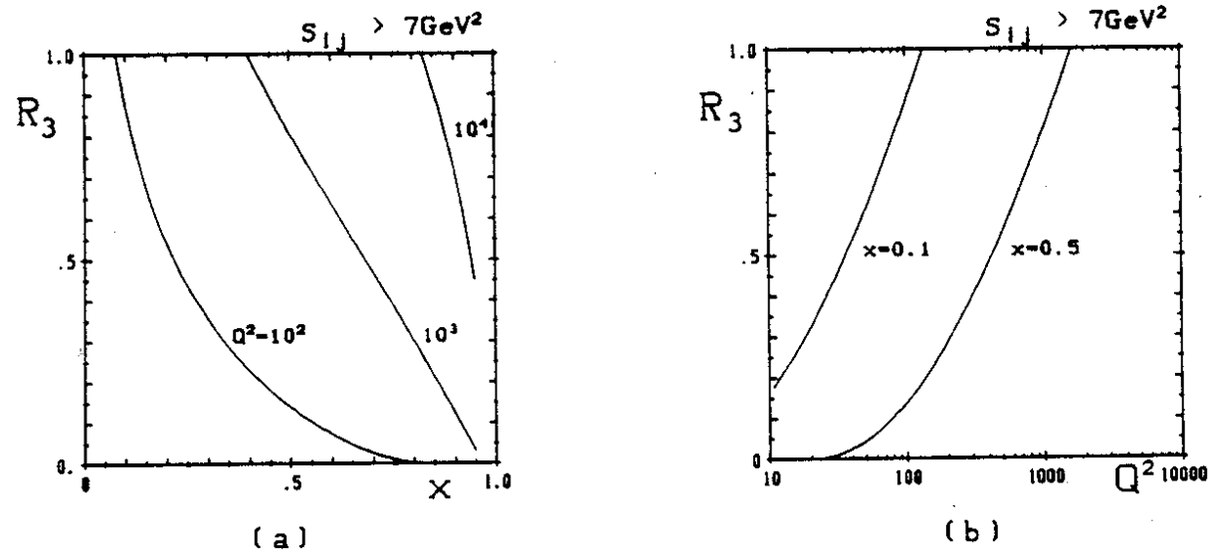

Figure Captions

Figure 1: a Zeroth order diagrams for lepton-parton scattering. b-d Real (tree graph) $O(\alpha_s)$ corrections: quark initiated (b), boson-gluon fusion (c), antiquark initiated (d). e Kinematic diagram for three-jet production.

Figure 2: $O(\alpha_s)$ K-factor for NC and CC $e^- p$ scattering at HERA cms energy ($\sqrt{s} = 314\,\mathrm{GeV}$) as a function of Q^2 for various values of x.

Figure 3: Genuine 3-jet region (shaded area) of the 3-parton phase space for various jet definition schemes and two different x-values. a W-scheme, b Q-scheme, c mixed-scheme.

Figure 4: The ratio R_3 of 3-jet events over the total $O(\alpha_s)$ cross section for the W-scheme as a function of x for various Q^2 and W^2 values and as a function of Q^2 for various x values.

Figure 5: The ratio R_3 of 3-jet events over the total $O(\alpha_s)$ cross section for the Q-scheme as a function of x for various Q^2 and W^2 values and as a function of Q^2 for various x values.

Figure 6: The ratio R_3 of 3-jet events over the total $O(\alpha_s)$ cross section for the mixed-scheme as a function of x for various Q^2 and W^2 values and as a function of Q^2 for various x values.

Figure 7: The ratio R_3 of 3-jet events over the total $O(\alpha_s)$ cross section for the W-scheme as a function of Q^2 for a given fixed coupling constant $\alpha_s(Q^2 = 300\mathrm{GeV}^2)$ and for a running coupling constant $\alpha_s(Q^2)$.

Figure 8: The ratio R_3 of 3-jet events over the total $O(\alpha_s)$ cross section for a jet definition scheme corresponding to the requirement $s_{ij} \geq 7\mathrm{GeV}^2$ as a function of x for various Q^2 values and as a function of Q^2 for various x values.

References

[APV78] D. Amati, R. Petronzio, G. Veneziano; Nucl. Phys. B140 (1978) 54; B146 (1978) 29

[AEM79] G. Altarelli, J.K. Ellis, G. Martinelli; Nucl. Phys. B157 (1979) 461

[AM78] G. Altarelli, G. Martinelli; Phys. Lett. 76B (1978) 89

[BIR87] P.N. Burrows, G. Ingelman, E. Ros; DESY preprint, DESY 87-167 (1987); Z. Phys. C in press

[BIS87] M. Bengtsson, G. Ingelman, T. Sjöstrand; DESY preprint, DESY 87-097 (1987); Nucl. Phys. B in press

[BS87] M. Bengtsson, T. Sjöstrand; Comput. Phys. Common. 43 (1987) 367

[BSZ86] M. Bengtsson, T. Sjöstrand, M. van Zijl; Z. Phys. C32 (1986) 67

[BG79] P. Binétruy, G. Giradi; Nucl. Phys. B155 (1979) 150

[BM77] P. Breitenlohner, D. Maison; Comm. Math. Phys. 52 (1977) 11

[CFP80] G. Curci, W. Furmanski, R. Petronzio; Nucl. Phys. B175 (1980) 27

[EGMPR79] R.K. Ellis, H. Georgi, M. Machacek, H.D. Politzer, G.C. Ross, Nucl. Phys. B152 (1979) 285

[EMC] J.J. Aubert et al., EMC Collaboration, Phys. Lett. 95B (1980) 306; Phys. Lett. 100B (1981) 433; Phys. Lett. 130B (1983) 118; M. Arneodo et al., EMC Collaboration, Phys. Lett. underline149B (1984) 415; CERN-EP/87-112 (1987)

[FKL81] E.G. Floratos, C. Kounnas, R. Lacazw; Phys. Lett. 98B (1981) 89; Phys. Lett. 98B (1981) 285; Nucl. Phys. B192 (1981) 417

[FP82] W. Furmanski, R. Petronzio; Z. Phys. C11 (1982) 293

[GHR82] M. Glück, E. Hoffmann and E. Reya; Z. Phys. C13 (1982) 119

[GS78] H. Georgi, J. Sheiman, Harvard preprint HUTP-78/A034 (1978)

[HHK82] K. Hagiwara, K. Hikasa, N. Kai; Univ. of Wisconsin-Madison preprint, MAD PH/47 (1982); Phys. Rev. Lett. 47 (1981) 983

[HW81] R.T. Herrod, S. Wada; Phys. Lett. 96B (1981) 195; Z. Phys. C9 (1981) 351

[In87] G. Ingelman, DESY preprint, DESY 87-114 (1987)

[In86] G. Ingelman, LEPTO 4.3, CERN program pool W5046 (1986); LEPTO 5.2, DESY preprint in preparation

[KR80] G. Kramer, Ch. Rumpf; Phys. Lett. 89B (1980) 380

[KR81] G. Kramer, Ch. Rumpf, J. Willrodt; Z. Phys. C7 (1981) 337

[KS87] G.A. Schuler, J.G. Körner; DESY preprint, DESY 87-124 (1987)

[KKLS85] J.G. Körner, G. Schuler, G. Kramer, B. Lampe; Phys. Lett. 164B (1985) 136

[KKLS86] J.G. Körner, G. Schuler, G. Kramer, B. Lampe; Z. Phys. C32 (1986) 181

[LS78] S.B. Libby, G. Sterman; Phys. Rev. D18 (1978) 3252

[Me78] A. Mendez; Nucl. Phys. B145 (1978) 199

[MW79] A. Mendez, T. Weiler; Phys. Lett. 83B (1979) 221

[Mo81] R. Moore; Nucl. Phys. B191 (1981) 113

[Mu78] A.M. Muller; Phys. Rev. D18 (1978) 3705

[PR80] R. D. Peccei, R. Rückl; Nucl. Phys. B162 (1980) 125

[RR79] J. Ranft, G. Ranft; Phys. Lett. 82B (1979) 129

[Sch87] G.A. Schuler; Nucl. Phys. B299 (1988) 21

[S150] P.M. Stevenson; Nucl. Phys. B150 (1979) 357

[S156] P.M. Stevenson; Nucl. Phys. B156 (1979) 43

[SW77] G. Sterman, S. Weinberg; Phys. Rev. Lett. 39 (1977) 1436

[Wo86] G. Wolf; DESY preprint, DESY 86-089 (1986)